QUANTUM TRAJECTORY APPROACH TO STATISTICS OF AMPLIFIED AND DAMPED CAVITY FIELDS

Teppo Häyrynen

Dissertation for the degree of Doctor of Science in Technology to be presented with due permission of the Faculty of Information and Natural Sciences for public examination and debate in auditorium D at Aalto University, School of Science and Technology (Espoo, Finland) on December 17th, 2010, at 12:30 p.m.

Author	Teppo Häyrynen

Name of the dissertation

Quantum trajectory approach to statistics of amplified and damped cavity fields

Abstract

Analysis of quantum optical experiments and the simulation of optical devices require detailed quantum mechanical models, especially in the case of weak optical fields. In this thesis the quantum dynamics of cavity fields are investigated and new tools for modeling cavity fields interacting with an energy reservoir are developed.

Using the quantum trajectory approach the field dynamics during photon detection processes are investigated. Two experimentally feasible detector models, the resolving and the non-resolving detector scheme, are derived and applied to single photon detection and coincidence photon detection experiments. Furthermore, equivalence of the cavity field model to the beam splitter based single photon subtraction and addition schemes is shown.

In addition to the detection schemes described above, a reduced model for fields in a non-ideal cavity interacting with a dissipative and amplifying reservoir through multiple two state systems is derived. The reduced model can be used to describe e.g. light emitting diodes and lasers depending on the relative strengths of the losses and energy injection. In these cases the model reproduces fields that approach a thermal or a coherent field, respectively.

The derived models can be applied to wide variety of cavity field experiments. The reduced field model can be applied to modeling the optical fields of semiconductor devices or to describe cavity field based quantum information processing experiments. Furthermore, fundamental quantum optics experiments of single photon addition, single photon subtraction, coincidence detection, and their combinations can be analyzed using the derived models.

A! Aalto-yliopisto

VÄITÖSKIRJAN TIIVISTELMÄ	AALTO-YLIOPISTO TEKNILLINEN KORKEAKOULU PL 11000, 00076 AALTO http://www.aalto.fi

Tekijä	Teppo Häyrynen

Väitöskirjan nimi

Quantum trajectory approach to statistics of amplified and damped cavity fields

Käsikirjoituksen päivämäärä	11.10.2010	Korjatun käsikirjoituksen päivämäärä	24.11.2010

Väitöstilaisuuden ajankohta	17.12.2010

☐ Monografia   ☒ Yhdistelmäväitöskirja (yhteenveto + erillisartikkelit)

Tiedekunta	Informaatio- ja luonnontieteiden tiedekunta
Laitos	Lääketieteellisen tekniikan ja laskennallisen tieteen laitos
Tutkimusala	Kvanttioptiikka
Vastaväittäjä(t)	Professori Igor Jex
Työn valvoja	Professori Jukka Tulkki
Työn ohjaaja	Professori Jukka Tulkki

Tiivistelmä

Kvanttioptisten kokeiden analysointi ja optisten komponenttien simulointi edellyttää tarkkojen kvanttimekaanisten mallien käyttämistä erityisesti heikkojen optisten kenttien tapauksessa. Tässä väitöskirjassa tutkitaan kaviteettikenttien kvanttidynamiikkaa ja kehitetään uusia malleja sellaisten kaviteettikenttien mallintamiseen, jotka on häviöllisesti kytketty ympäristöönsä ja joihin pumpataan samanaikaisesti energiaa.

Optisen kentän dynamiikkaa fotonien mittauksen aikana tutkitaan kvanttipolkumenetelmää hyödyntäen. Väitöskirjassa johdetaan kaksi kokeellisesti toteuttamiskelpoista detektorimallia: RD-malli ja NRD-malli. RD-malli kuvaa detektoreita, jotka pystyvät havaitsemaan yksittäisen fotonin ja erottelemaan jokaisen detektorin absorboiman fotonin. NRD-malli puolestaan kuvaa detektoreita, jotka pystyvät havaitsemaan yksittäisen fotonin, mutta eivät pysty erottelemaan, onko fotoneita absorboitu yksi vai useampia. Näitä malleja sovelletaan yksittäisen mittauksen mallintamiseen sekä koinsidenssimittauksen mallintamiseen. Lisäksi osoitetaan kaviteettimallin yhtenevyys säteenjakajamalliin yhden fotonin luomis- ja tuhoamiskokeissa.

Edelläkuvattujen mittausten mallintamisen lisäksi väitöskirjassa johdetaan redusoitu malli sellaisille kaviteettikentille, jotka vuorovaikuttavat energialähteen ja energianielun kanssa useiden kaksitasosysteemien välityksellä. Riippuen vahvistuksen ja häviöiden keskinäisestä suhteesta redusoitua mallia voidaan käyttää esimerkiksi loistediodien ja lasereiden mallintamiseen. Tällöin malli tuottaa vastaavasti termisen ja koherentin optisen kentän.

Väitöskirjassa johdettuja malleja voidaan soveltaa esimerkiksi optisten puolijohdekomponenttien kentän mallintamiseen sekä kaviteettia hyödyntävien kvanttimekaanisten informaatioprosessointikokeiden mallintamiseen. Lisäksi malleja voidaan käyttää perustavanlaatuisten kvanttioptisten kokeiden, kuten yhden fotonin luominen, yhden fotonin tuhoaminen, koinsidenssimittausten ja näiden yhdistelmien, kuvaamiseen.

Asiasanat	Dynaaminen kaviteettikentän malli, fotonien havaitseminen, CQED

ISBN (painettu)	978-952-60-3520-8	ISSN (painettu)	1797-3996
ISBN (pdf)	978-952-60-3521-5	ISSN (pdf)	
Kieli	Englanti	Sivumäärä	87s. + liitteet 62 s.

Julkaisija	Lääketieteellisen tekniikan ja laskennallisen tieteen laitos

Painetun väitöskirjan jakelu	Lääketieteellisen tekniikan ja laskennallisen tieteen laitos

☒ Luettavissa verkossa osoitteessa http://lib.tkk.fi/Diss/

Preface

This thesis for the degree of Doctor of Science (Technology) is the result of the work done in the Department of Biomedical Engineering and Computational Science at Aalto University during the years 2003–2010. The work has been partly funded by Graduate School of Electrical and Communications Engineering and Multidisciplinary Institute of Digitalisation and Energy (MIDE). I also acknowledge the support of Ulla Tuominen Foundation (Ulla Tuomisen säätiö).

Furthermore, I would like to express my gratitude to my supervisor Professor Jukka Tulkki for his guidance and encouragement and to my closest colleagues for the inspiring work environment. Finally, I wish to thank my family for their support.

Contents

x

List of Publications

This thesis consists of an overview and of the following publications which are referred to in the text by their Roman numerals.

I   T. Häyrynen, J. Oksanen and J. Tulkki, *On the origin of divergences in the coincidence probabilities in cavity photodetection experiments*, Journal of Physics B: Atomic, Molecular and Optical Physics **42**, 145506 (2009).

II   T. Häyrynen, J. Oksanen and J. Tulkki, *Exact theory for photon subtraction for fields from quantum to classical limit*, EPL **87**, 44002 (2009).

III   T. Häyrynen, J. Oksanen and J. Tulkki, *Derivation of generalized quantum jump operators and comparison of the microscopic single photon detector models*, The European Physical Journal D **56**, pp. 113–121 (2010).

IV   T. Häyrynen, J. Oksanen and J. Tulkki, *Unified quantum jump superoperator for optical fields from the weak- to the strong-coupling limit*, Physical Review A **81**, 063804 (2010).

V   T. Häyrynen, J. Oksanen and J. Tulkki, *Quantum trajectory model for photon detectors and optoelectronic devices*, 17th CEWQO 2010 Topical issue of Physica Scripta, accepted (2010).

VI   T. Häyrynen, J. Oksanen and J. Tulkki, *Dynamics of cavity fields with dissipative and amplifying couplings through multiple quantum two state systems*, Physical Review A, accepted (2010)

Author's contribution

This dissertation is composed of six publications and introduction to the fundamental underlying theory. T. Häyrynen has been the main author in all of the publications. He has performed all derivations and calculations involved in the publications and written the first versions of the manuscripts. Prof. Jukka Tulkki and Dr. Tech. Jani Oksanen have given valuable feedback and guidance throughout this process.

List of Abbreviations

APD   Avalanche photo diode

BS   Beam splitter

CP   Coincidence probability

LED   Light emitting diode

LO   Local oscillator

NRD   Non-resolving detector

PMT   Photomultiplier tube

QJS   Quantum jump superoperator

RD   Resolving detector

List of symbols

γ	Field-two state system coupling
γ_{sd}	Model parameter of the SD model
γ_e	Model parameter of the E model
ε	Permeability of a material
ε_0	Permeability of the vacuum
$\varepsilon_{\mathbf{k}}$	Unit polarization vector
θ	Beam splitter parameter
λ_A	Amplifying coupling of a two state system into the reservoir
λ_D	Dissipative coupling of a two state system into the reservoir
μ	Permittivity of a material
μ_0	Permittivity of the vacuum
ξ	Coupling of the optical field to the thermal reservoir
$\hat{\rho}$	Density operator
$\hat{\sigma}_-$	De-excitation operator of the two state system
$\hat{\sigma}_+$	Excitation operator of the two state system
ω	Angular frequency
$\mathbf{A}$	Vector potential
$\hat{\mathbf{A}}$	Vector potential operator
A_A	Amplification factor
A_D	Dissipation factor
$\hat{a}$	Photon annihilation operator
$\hat{a}^\dagger$	Photon creation operator
$\mathbf{B}$	Magnetic flux density vector
$\hat{\mathbf{B}}_{\mathbf{k}}$	Magnetic field operator
B	Saturation factor
$\hat{B}$	Beam splitter operator
C	Mirror losses

$\hat{C}(t,m)$	Operator corresponding to detection of m photons during $[0,t)$
$\hat{C}_{\mathrm{NRD}}(t)$	Operator of non-resolving detection during $[0,t)$
$\hat{C}_{\mathrm{RD}}(t)$	Operator of single photon resolving detection during $[0,t)$
c_0	Speed of light in vacuum
$\mathbf{D}$	Electric Displacement vector
$\mathbf{E}$	Electric field vector
$\hat{\mathbf{E}}_{\mathbf{k}}$	Electric field operator
$E_{F,e}$	Quasi-Fermi level of electrons
$E_{F,h}$	Quasi-Fermi level of holes
$|e\rangle$	Excited state
f_e	Fermi function for electrons
f_h	Fermi function for holes
$G^{(n)}$	n^{th} order correlation function
$g^{(n)}$	n^{th} order coherence degree
$|g\rangle$	Ground state
$\mathbf{H}$	Magnetic field vector
$\mathcal{H}$	Hamiltonian operator
$\hbar$	Planck's constant
$\hat{J}$	Quantum jump superoperator
$\mathbf{k}$	Wavevector
k	Absolute value of the wavevector, $|\mathbf{k}|$
k_B	Boltzmann's constant
N_s	Number of two state systems
$\bar{n}_{th}$	Number of photons in the thermal reservoir
$\hat{S}$	No-jump superoperator
R	Reflection coefficient
$\mathbf{r}$	Position vector
r_D	Dissipation rate
r_A	Energy injection rate
T	Temperature

T	Transmission coefficient
$\hat{T}_t$	Average evolution operator during $[0, t)$
W	Semiconductor-field coupling

1 Introduction

Quantum optics and especially the quantum theory of coherence started to develop during 1950s after Hanbury Brown and Twiss [1] measured the correlation of photons in two coherent light beams using beam splitters and photomultiplier tubes. After the experiment the quantum theory of optical coherence was developed greatly by Glauber [2, 3]. Although the first steps of quantum optics were taken decades ago, many recent quantum optical experiments still depend on beam splitters and photodetectors. For example, by using a light source, a beam splitter and photodetectors, Parigi *et al.* [4] recently showed that after subtracting a single photon from a light field the expectation value of the number of the photons may be twice the initial value. Cavity quantum optics is also a subject of great interest since it may offer a way to quantum information processing applications [5].

Analysis of quantum optical experiments and the simulation of optical devices require detailed quantum mechanical models, especially in the case of weak optical fields. In this summary and related publications the quantum dynamics of cavity fields are investigated and new tools for modeling cavity fields interacting with an energy reservoir are developed.

In general the results described in the publications are based on applying the quantum trajectory approach to investigate e.g. how the measurement of a photon will change the cavity field. In publications I and II two different experimentally feasible detector models, the resolving detector corresponding to detection of exactly one photon and the non-resolving detector corresponding to detection of at least one photon, are derived and analyzed. In contrast to the previous studies, which have only been applicable for either weak or strong coupling of the field and the detector, we have derived models that are applicable also for intermediate coupling. With the use of these detector models we analyze the coincidence photon detection

experiments and also consider the photon bunching and anti-bunching phenomena for selected initial states of the field.

In publications II and V we analyze single photon addition and subtraction experiments based on light pulses incident on a beam splitter by using the detector schemes introduced. We show that by relating the transmission and reflection probabilities of the beam splitter model to the cavity field-detector coupling and to the interaction time of our model, the models become equivalent.

In addition to the cavity field detection, in publications IV, V and VI we analyze setups where the cavity field is coupled to an energy source and an energy drain through one or multiple two state systems. We derive a reduced field model which captures the effect of the energy reservoir by the strengths of the coupling between the field and the two state system and the coupling of the two state system and the reservoir. By taking the mirror losses of the cavity into account, we show that our setup can operate as a light emitting diode or as a laser. We also show that our model can be applied to analyze the optical fields of semiconductor devices.

In this summary the necessary prerequisites and selected topics of the attached publications are discussed.

2 Quantum optical field

2.1 Quantization of the electromagnetic field

Quantized description of electromagnetic field is obtained from the classical theory. As a brief introduction to the topics of this thesis we demonstrate the analogy between the classical and the quantized fields for the simplest case of vacuum. We start from the classical description of electromagnetic field using the Maxwell's equations, which relate the electric and magnetic fields $\mathbf{E}$ and $\mathbf{H}$ to the electric displacement $\mathbf{D}$ and to the magnetic flux density $\mathbf{B}$. Maxwell's equations for the vacuum are given by [6–8]

$$\nabla \times \mathbf{H} = \frac{\partial \mathbf{D}}{\partial t} \tag{2.1}$$

$$\nabla \times \mathbf{E} = -\frac{\partial \mathbf{B}}{\partial t} \tag{2.2}$$

$$\nabla \cdot \mathbf{B} = 0 \tag{2.3}$$

$$\nabla \cdot \mathbf{D} = 0, \tag{2.4}$$

where we have assumed that charge and current densities are zero. Furthermore, the constitutive relations give

$$\mathbf{B} = \mu_0 \mathbf{H} \tag{2.5}$$

$$\mathbf{D} = \varepsilon_0 \mathbf{E}, \tag{2.6}$$

where μ_0 and ε_0 are the permittivity and permeability of the vacuum which relate to the speed of light as $c_0 = 1/\sqrt{\mu_0 \varepsilon_0}$. Since it holds for every vector function $\mathbf{f}(\mathbf{r})$ that $\nabla \cdot (\nabla \times \mathbf{f}(\mathbf{r})) = 0$ equation (2.3) is satisfied if we define the magnetic flux density using a vector potential function as $\mathbf{B} = \nabla \times \mathbf{A}$. Substituting this into (2.2) gives $\nabla \times (\mathbf{E} + \frac{\partial}{\partial t}\mathbf{A}) = 0$ and accordingly $\mathbf{E} = -\frac{\partial}{\partial t}\mathbf{A}$. From equation (2.1) we obtain $\nabla \times \nabla \times \mathbf{A} = \mu_0 \varepsilon_0 \frac{\partial^2}{\partial t^2}\mathbf{A}$, where $\nabla \times \nabla \times \mathbf{A} = \nabla(\nabla \cdot \mathbf{A}) - \nabla^2 \mathbf{A}$. By the use of vector potential $\mathbf{A}$ in the Coulomb gauge $\nabla \cdot \mathbf{A} = 0$ the Maxwell's equation give

the following wave equation for the vector potential

$$\frac{\partial^2}{\partial t^2}\mathbf{A} - c_0^2 \nabla^2 \mathbf{A} = 0 \tag{2.7}$$

$$\mathbf{E} = -\frac{\partial}{\partial t}\mathbf{A} \tag{2.8}$$

$$\mathbf{B} = \nabla \times \mathbf{A}. \tag{2.9}$$

The electromagnetic field will be now quantized by transforming the vector potential $\mathbf{A}$ to vector potential operator $\hat{\mathbf{A}}$.

In a cube with side of L the vector potential can be expanded using planewaves and their Fourier series as

$$\mathbf{A} = \sum_{\mathbf{k}}[\mathbf{A_k}(t)e^{i\mathbf{k}\cdot\mathbf{r}} + \mathbf{A_k^*}(t)e^{-i\mathbf{k}\cdot\mathbf{r}}], \tag{2.10}$$

where, using the periodic boundary conditions, $k_i = 2\pi\nu_i/L$, with $i = x, y, z$ and $\nu_i = 0, \pm 1, \pm 2, \ldots$. For each wave vector $\mathbf{k}$ there is two independent polarizations as will be shown later. These two possibilities are included in the summation $\sum_{\mathbf{k}}$. In a more general case the solutions of the wave equation (2.7) (i.e. the normal modes) are used instead of the plane waves and, furthermore, the vacuum parameters ε_0 and μ_0 are replaced with the material parameters ε and μ.

The Coulomb gauge condition, $\nabla \cdot \mathbf{A}(t) = 0$, is satisfied if $\mathbf{k} \cdot \mathbf{A_k}(t) = \mathbf{k} \cdot \mathbf{A_k^*}(t) = 0$. Thus, the Fourier component $\mathbf{A_k}$ is perpendicular to the wavevector $\mathbf{k}$. Substitution of the Fourier expansion into the wave equation (2.7) gives for each mode $\mathbf{k}$

$$k^2\mathbf{A_k}(t) + \frac{1}{c_0^2}\frac{\partial^2 \mathbf{A_k}(t)}{\partial t^2} = 0 \tag{2.11}$$

$$\partial^2 \mathbf{A_k}(t)/\partial t^2 = -\omega_{\mathbf{k}}^2 \mathbf{A_k}(t) \tag{2.12}$$

where $\omega_{\mathbf{k}} = c_0 k$. The solution is

$$\mathbf{A_k}(t) = \mathbf{A_k}e^{-i\omega_{\mathbf{k}}t}, \tag{2.13}$$

and corresponding equations hold for $\mathbf{A_k^*}(t)$. The vector potential can now be written as

$$\mathbf{A} = \sum_{\mathbf{k}}[\mathbf{A_k}e^{i\mathbf{k}\cdot\mathbf{r}-i\omega_{\mathbf{k}}t} + \mathbf{A_k^*}e^{-i\mathbf{k}\cdot\mathbf{r}+i\omega_{\mathbf{k}}t}]. \tag{2.14}$$

The energy of the classical mode $\mathbf{k}$ is given by Hamiltonian [6,7]

$$H_{\mathbf{k}} = \frac{1}{2} \int_V \left(\varepsilon_0 |\mathbf{E_k}|^2 + \mu_0^{-1} |\mathbf{B_k}|^2 \right) \mathrm{d}V = 2\varepsilon_0 V \omega_{\mathbf{k}}^2 |\mathbf{A_k}|^2. \tag{2.15}$$

Next we write the mode variables $\mathbf{A_k}$ and $\mathbf{A_k^*}$ using a generalized mode position coordinate $Q_{\mathbf{k}}$ and mode momentum coordinate $P_{\mathbf{k}}$ as

$$\mathbf{A_k} = \frac{\omega_{\mathbf{k}} Q_{\mathbf{k}} + \mathrm{i} P_{\mathbf{k}}}{\sqrt{4\varepsilon_0 V \omega_{\mathbf{k}}^2}} \varepsilon_{\mathbf{k}} \tag{2.16}$$

$$\mathbf{A_k^*} = \frac{\omega_{\mathbf{k}} Q_{\mathbf{k}} - \mathrm{i} P_{\mathbf{k}}}{\sqrt{4\varepsilon_0 V \omega_{\mathbf{k}}^2}} \varepsilon_{\mathbf{k}}, \tag{2.17}$$

where $\varepsilon_{\mathbf{k}}$ is the polarization vector. It follows from the Maxwell's equations that $\mathbf{k} \cdot \varepsilon_{\mathbf{k}} = 0$ i.e. the fields are transverse and there are two independent polarization directions for each wavevector $\mathbf{k}$. Using equations (2.16) and (2.17), the Hamiltonian (2.15) simplifies to

$$H_{\mathbf{k}} = \frac{1}{2} \left(P_{\mathbf{k}}^2 + \omega_{\mathbf{k}}^2 Q_{\mathbf{k}}^2 \right). \tag{2.18}$$

This form corresponds to the energy of a classical harmonic oscillator. For comparison, the Hamiltonian operator of a one dimensional quantum mechanical harmonic oscillator with unit mass is

$$\mathcal{H} = \frac{1}{2}(\hat{p}^2 + \omega^2 \hat{q}^2), \tag{2.19}$$

where $\hat{p}$ is the position operator and $\hat{q}$ is the momentum operator obeying the commutation relation $[\hat{q}, \hat{p}] = \mathrm{i}\hbar$. The annihilation and creation operators are defined using a canonical transformation as

$$\hat{a} = \frac{1}{\sqrt{2\hbar\omega}}(\omega\hat{q} + \mathrm{i}\hat{p}) \tag{2.20}$$

$$\hat{a}^\dagger = \frac{1}{\sqrt{2\hbar\omega}}(\omega\hat{q} - \mathrm{i}\hat{p}) \tag{2.21}$$

$$\hat{q} = \sqrt{\frac{\hbar}{2\omega}}(\hat{a} + \hat{a}^\dagger) \tag{2.22}$$

$$\hat{p} = -\mathrm{i}\sqrt{\frac{\hbar\omega}{2}}(\hat{a} - \hat{a}^\dagger). \tag{2.23}$$

The annihilation and creation operators obey the commutation relation $[\hat{a}, \hat{a}^\dagger] = 1$.

The similarity of the classical Hamiltonian (2.18) and the quantum mechanical Hamiltonian (2.19) allows quantization of the electromagnetic field by replacing variables $P_{\mathbf{k}}$ and $Q_{\mathbf{k}}$ with operators $\hat{p}_{\mathbf{k}}$ and $\hat{q}_{\mathbf{k}}$ in equations (2.16) and (2.17) giving

$$\hat{\mathbf{A}}_{\mathbf{k}} \;=\; \frac{1}{\sqrt{4\varepsilon_0 V \omega_{\mathbf{k}}^2}}(\omega_{\mathbf{k}}\hat{q}_{\mathbf{k}} + \mathrm{i}\hat{p}_{\mathbf{k}})\varepsilon_{\mathbf{k}} = \sqrt{\frac{\hbar}{2\varepsilon_0 V \omega_{\mathbf{k}}}}\hat{a}_{\mathbf{k}}\varepsilon_{\mathbf{k}} \tag{2.24}$$

$$\hat{\mathbf{A}}_{\mathbf{k}}^* \;=\; \frac{1}{\sqrt{4\varepsilon_0 V \omega_{\mathbf{k}}^2}}(\omega_{\mathbf{k}}\hat{q}_{\mathbf{k}} - \mathrm{i}\hat{p}_{\mathbf{k}})\varepsilon_{\mathbf{k}} = \sqrt{\frac{\hbar}{2\varepsilon_0 V \omega_{\mathbf{k}}}}\hat{a}_{\mathbf{k}}^\dagger\varepsilon_{\mathbf{k}}. \tag{2.25}$$

The vector potential, electric field, and magnetic field operators associated to mode $\mathbf{k}$ are

$$\hat{\mathbf{A}}_{\mathbf{k}} \;=\; \sqrt{\frac{\hbar}{2\varepsilon_0 V \omega_{\mathbf{k}}}}\varepsilon_{\mathbf{k}}[\hat{a}_{\mathbf{k}}\exp(-\mathrm{i}\omega_{\mathbf{k}}t + \mathrm{i}\mathbf{k}\cdot\mathbf{r}) + \hat{a}_{\mathbf{k}}^\dagger\exp(\mathrm{i}\omega_{\mathbf{k}}t - \mathrm{i}\mathbf{k}\cdot\mathbf{r})] \tag{2.26}$$

$$\hat{\mathbf{E}}_{\mathbf{k}} \;=\; \mathrm{i}\sqrt{\frac{\hbar\omega_{\mathbf{k}}}{2\varepsilon_0 V}}\varepsilon_{\mathbf{k}}[\hat{a}_{\mathbf{k}}\exp(-\mathrm{i}\omega_{\mathbf{k}}t + \mathrm{i}\mathbf{k}\cdot\mathbf{r}) - \hat{a}_{\mathbf{k}}^\dagger\exp(\mathrm{i}\omega_{\mathbf{k}}t - \mathrm{i}\mathbf{k}\cdot\mathbf{r})] \tag{2.27}$$

$$\hat{\mathbf{B}}_{\mathbf{k}} \;=\; \mathrm{i}\sqrt{\frac{\hbar}{2\varepsilon_0 V \omega_{\mathbf{k}}}}\mathbf{k}\times\varepsilon_{\mathbf{k}}[\hat{a}_{\mathbf{k}}\exp(-\mathrm{i}\omega_{\mathbf{k}}t + \mathrm{i}\mathbf{k}\cdot\mathbf{r}) - \hat{a}_{\mathbf{k}}^\dagger\exp(\mathrm{i}\omega_{\mathbf{k}}t - \mathrm{i}\mathbf{k}\cdot\mathbf{r})], \tag{2.28}$$

where $\varepsilon_{\mathbf{k}}$ is the polarization unit vector of mode $\mathbf{k}$. Different modes are orthogonal solutions of the wave equation. The operator operating into mode $\mathbf{k}$ is denoted by subscript $\mathbf{k}$. Thus $\hat{a}_{\mathbf{k}}^\dagger$ creates and $\hat{a}_{\mathbf{k}}$ destructs a photon with energy $\hbar\omega_{\mathbf{k}}$ in the electromagnetic field mode $\mathbf{k}$ of the cavity. Furthermore, the operators of the total vector potential, the transverse electric field, and the transverse magnetic field are $\hat{\mathbf{A}} = \sum_{\mathbf{k}}\hat{\mathbf{A}}_{\mathbf{k}}$, $\hat{\mathbf{E}} = \sum_{\mathbf{k}}\hat{\mathbf{E}}_{\mathbf{k}}$ and $\hat{\mathbf{B}} = \sum_{\mathbf{k}}\hat{\mathbf{B}}_{\mathbf{k}}$. The electric field operator is divided into two parts

$$\hat{\mathbf{E}}(\mathbf{r}, t) \;=\; \hat{\mathbf{E}}^{(+)}(\mathbf{r}, t) + \hat{\mathbf{E}}^{(-)}(\mathbf{r}, t) \tag{2.29}$$

$$\hat{\mathbf{E}}^{(+)}(\mathbf{r}, t) \;=\; \mathrm{i}\sum_{\mathbf{k}}\sqrt{\frac{\hbar\omega_{\mathbf{k}}}{2\varepsilon_0 V}}\varepsilon_{\mathbf{k}}\hat{a}_{\mathbf{k}}\exp(-\mathrm{i}\omega_{\mathbf{k}}t + \mathrm{i}\mathbf{k}\cdot\mathbf{r}) \tag{2.30}$$

$$\hat{\mathbf{E}}^{(-)}(\mathbf{r}, t) \;=\; -\mathrm{i}\sum_{\mathbf{k}}\sqrt{\frac{\hbar\omega_{\mathbf{k}}}{2\varepsilon_0 V}}\varepsilon_{\mathbf{k}}\hat{a}_{\mathbf{k}}^\dagger\exp(\mathrm{i}\omega_{\mathbf{k}}t - \mathrm{i}\mathbf{k}\cdot\mathbf{r}), \tag{2.31}$$

where $\hat{\mathbf{E}}^{(+)}$ is called the positive and $\hat{\mathbf{E}}^{(-)}$ the negative frequency part. Similar equations hold for the magnetic field operator.

2.2   Density operator formalism

The density operator formalism is shortly introduced since we will apply it in all the analytical and numerical calculations represented in this thesis.

In quantum mechanics a state of a pure system at time t is described with a state vector $|\Psi(t)\rangle$. Let us assume that Hamiltonian operator describing the energy of the system is $\mathcal{H}$. The time development of the system is governed by the Schrödinger equation [9]

$$\mathcal{H}|\Psi(t)\rangle = i\hbar\frac{\mathrm{d}}{\mathrm{d}t}|\Psi(t)\rangle, \tag{2.32}$$

which has a formal solution

$$|\Psi(t)\rangle = e^{-i\mathcal{H}t/\hbar}|\Psi(0)\rangle. \tag{2.33}$$

A statistical ensemble or a system interacting with its environment (i.e. coupled systems) cannot usually be described by a state vector. Instead the density operator formalism [6, 9, 10] must be used.

For a pure state $|\Psi(t)\rangle$ a density operator is defined as

$$\hat{\rho}(t) = |\Psi(t)\rangle\langle\Psi(t)|. \tag{2.34}$$

If the state is a superposition state $|\Psi(t)\rangle = \sum_{i=0}^{\infty} \psi_i(t)|i\rangle$ the density operator can be written as

$$\hat{\rho}(t) = |\Psi(t)\rangle\langle\Psi(t)| = \sum_{i=0,j=0}^{\infty} \psi_i(t)\psi_j^*(t)|i\rangle\langle j| = \sum_{i=0,j=0}^{\infty} \rho_{i,j}|i\rangle\langle j|. \tag{2.35}$$

Note that, although we used a state vector to define the density operator, the formalism is more general. The density operator can also be defined for systems that cannot be represented by a state vector.

A trace of the density operator is defined as $\mathrm{Tr}\{\hat{\rho}\} = \sum_{k=0}^{\infty}\langle k|\left(\sum_{i=0,j=0}^{\infty}\rho_{i,j}|i\rangle\langle j|\right)|k\rangle$ $= \sum_{i=0}^{\infty}\rho_{i,i} = 1$, where $\rho_{i,i}$ is the probability of the state $|i\rangle$ in the mixed state. For a

pure state $\hat{\rho}^2 = \hat{\rho}$ and $\text{Tr}\{\hat{\rho}^2\} = \sum_{i=0}^{\infty} \rho_{i,i}^2 = 1$. The expectation value of a quantum mechanical operator $\hat{A}$ operating on a mixed state is further given by

$$\langle \hat{A} \rangle = \text{Tr}\{\hat{A}\hat{\rho}\} = \sum_{i=0}^{\infty} \rho_{i,i} \langle i|\hat{A}|i \rangle. \tag{2.36}$$

Using the Schrödinger equation an equation of motion for the density operator is obtained as

$$\frac{\mathrm{d}}{\mathrm{d}t}\hat{\rho}(t) = \left(\frac{\mathrm{d}}{\mathrm{d}t}|\Psi(t)\rangle\right)\langle\Psi(t)| + |\Psi(t)\rangle\left(\frac{\mathrm{d}}{\mathrm{d}t}\langle\Psi(t)|\right) = -\frac{\mathrm{i}}{\hbar}\left[\mathcal{H}, \hat{\rho}(t)\right], \tag{2.37}$$

where $[\hat{a}, \hat{b}] = \hat{a}\hat{b} - \hat{b}\hat{a}$ is the commutator. Equation (2.37) is called the Liouville-von Neumann equation [11, 12] and it has a formal solution

$$\hat{\rho(t)} = e^{-\mathrm{i}\mathcal{H}t/\hbar}\hat{\rho}(0)e^{\mathrm{i}\mathcal{H}t/\hbar}. \tag{2.38}$$

2.3 Examples of optical fields

2.3.1 Fock state

A Fock state, also called a number state, is a pure state describing a field having precisely n photons and is denoted as $\Psi_{\text{Fock}} = |n_{\mathbf{k}}\rangle$. Fock states are eigenstates of the number operator $\hat{n} = \hat{a}^{\dagger}\hat{a}$. The single mode density operator for a Fock state is

$$\hat{\rho}_{\text{Fock}} = |n_{\mathbf{k}}\rangle\langle n_{\mathbf{k}}|, \tag{2.39}$$

where the wavevector $\mathbf{k}$ denotes the mode. In single mode case it is usually omitted. The frequency of the mode is $\omega_{\mathbf{k}} = ck$, where $k = |\mathbf{k}|$. The density operator of multimode Fock field is

$$\hat{\rho}_{\text{Fock}} = |\{n_{\mathbf{k}}\}\rangle\langle\{n_{\mathbf{k}}\}| = |n_{\mathbf{k}_1}\rangle|n_{\mathbf{k}_2}\rangle|n_{\mathbf{k}_3}\rangle\ldots\langle n_{\mathbf{k}_3}|\langle n_{\mathbf{k}_2}|\langle n_{\mathbf{k}_1}|. \tag{2.40}$$

2.3.2   Coherent field

The coherent states, also called Glauber states, are the eigenstates of the annihilation operator so that $\hat{a}_k|\alpha_\mathbf{k}\rangle = \alpha_\mathbf{k}|\alpha_\mathbf{k}\rangle$. They are related to the number states (Fock states) as follows [2, 6]

$$\Psi_{\text{coh}} = |\alpha_\mathbf{k}\rangle = \exp(-\frac{1}{2}|\alpha_\mathbf{k}|^2) \sum_{n_\mathbf{k}=0}^{\infty} \frac{\alpha_\mathbf{k}^{n_\mathbf{k}}}{\sqrt{n_\mathbf{k}!}}|n_\mathbf{k}\rangle. \tag{2.41}$$

Single mode density operator for the coherent field is

$$\hat{\rho}_{\text{coh}} = |\alpha_\mathbf{k}\rangle\langle\alpha_\mathbf{k}| = \exp(-|\alpha_\mathbf{k}|^2) \sum_{n_\mathbf{k},m_\mathbf{k}=0}^{\infty} \frac{\alpha_\mathbf{k}^{n_\mathbf{k}}(\alpha_\mathbf{k}^*)^{m_\mathbf{k}}}{\sqrt{n_\mathbf{k}!m_\mathbf{k}!}}|n_\mathbf{k}\rangle\langle m_\mathbf{k}|. \tag{2.42}$$

Parameter $|\alpha_\mathbf{k}|^2 = \langle\alpha_\mathbf{k}|\hat{a}_\mathbf{k}^\dagger\hat{a}_\mathbf{k}|\alpha_\mathbf{k}\rangle = \text{Tr}\{\hat{a}_\mathbf{k}^\dagger\hat{a}_\mathbf{k}\hat{\rho}_{\text{coh}}\}$ gives the mean number of photons in mode $\mathbf{k}$. Furthermore, the probability of finding n photons in that mode is $|\langle n_\mathbf{k}|\alpha_\mathbf{k}\rangle|^2 = e^{-|\alpha_\mathbf{k}|^2}\frac{|\alpha_\mathbf{k}|^{2n_\mathbf{k}}}{n_\mathbf{k}!}$. The density operator of a multimode coherent field is

$$\hat{\rho} = |\{\alpha_\mathbf{k}\}\rangle\langle\{\alpha_\mathbf{k}\}| = |\alpha_{\mathbf{k}_1}\rangle|\alpha_{\mathbf{k}_2}\rangle|\alpha_{\mathbf{k}_3}\rangle\ldots\langle\alpha_{\mathbf{k}_3}|\langle\alpha_{\mathbf{k}_2}|\langle\alpha_{\mathbf{k}_1}|. \tag{2.43}$$

2.3.3   Thermal field

The density operator for a single mode thermal, or chaotic, field is given by [6]

$$\hat{\rho}_{\text{ther}} = \sum_{n_\mathbf{k}=0}^{\infty} \frac{(\bar{n}_\mathbf{k})^{n_\mathbf{k}}}{(\bar{n}_\mathbf{k}+1)^{n_\mathbf{k}+1}}|n_\mathbf{k}\rangle\langle n_\mathbf{k}| = \sum_{n_\mathbf{k}=0}^{\infty} p_{n_\mathbf{k}}|n_\mathbf{k}\rangle\langle n_\mathbf{k}|, \tag{2.44}$$

where the mean photon number depends on temperature T and frequency of the field as

$$\bar{n}_\mathbf{k} = \frac{1}{\exp\left(\frac{\hbar\omega_\mathbf{k}}{k_B T}\right) - 1}, \tag{2.45}$$

where k_B is the Boltzmann's coefficient. The multimode density operator is given by

$$\hat{\rho}_{\text{ther}} = \sum_{\{n_\mathbf{k}\}=0}^{\infty} |\{n_\mathbf{k}\}\rangle\langle\{n_\mathbf{k}\}| \prod_\mathbf{k} \frac{(\bar{n}_\mathbf{k})^{n_\mathbf{k}}}{(\bar{n}_\mathbf{k}+1)^{n_\mathbf{k}+1}}. \tag{2.46}$$

2.4   Interaction of quantized field with a two state system

The interaction of quantized optical field with an atom (or an atom-like two state quantum system) where only a single electron interacts with the field can be described by a Hamiltonian [6, 7, 13]

$$\mathcal{H} = \mathcal{H}_{\text{atom}} + \mathcal{H}_{\text{field}} + \mathcal{H}_{\text{int}}. \tag{2.47}$$

Here the atomic Hamiltonian is

$$\mathcal{H}_{\text{atom}} = \hbar\omega_g |g\rangle\langle g| + \hbar\omega_e |e\rangle\langle e|, \tag{2.48}$$

where $|g\rangle$ and $|e\rangle$ are the ground state and the excited state of the two level system with respective energies of $\hbar\omega_g$ and $\hbar\omega_e$. It is usually written that $\hbar\omega_e = -\hbar\omega_g = \hbar\omega_0/2$, where $\hbar\omega_0$ is the energy difference of the two states. Therefore, the atomic Hamiltonian can be written as

$$\mathcal{H}_{\text{atom}} = \frac{1}{2}\hbar\omega_0\hat{\sigma}_0, \tag{2.49}$$

where $\hat{\sigma}_0 = |e\rangle\langle e| - |g\rangle\langle g|$. The field Hamiltonian in equation (2.47) is

$$\mathcal{H}_{\text{field}} = \hbar\omega\hat{a}^\dagger\hat{a}, \tag{2.50}$$

where ω is the frequency of the field and $\hbar\omega$ is the energy of a single photon. In the resonant case the frequency of the field corresponds to the energy difference of the excited and the ground states of the two level system. In the following we will assume exact resonance i.e. $\omega_0 = \omega$. Operators $\hat{a}$ and $\hat{a}^\dagger$ in equation (2.50) are the photon annihilation and creation operators of the field. The number operator $\hat{n} = \hat{a}^\dagger\hat{a}$ gives the number of photons in the field. We have dropped the zero point energy from Hamiltonian (2.50), since in our calculations only the energy difference, not the zero point, has significance. The Hamiltonian with the zero point energy is $\hbar\omega(\hat{n} + 1/2)$ which is obtained by substituting equations (2.22)–(2.23) into Hamiltonian (2.19). Finally, the interaction Hamiltonian, using the rotating wave and the dipole approximations, is

$$\mathcal{H}_{\text{int}} = \hbar\gamma\left(\hat{a}\hat{\sigma}_+ + \hat{a}^\dagger\hat{\sigma}_-\right), \tag{2.51}$$

where $\hat{\sigma}_+ = |e\rangle\langle g|$ and $\hat{\sigma}_- = |g\rangle\langle e|$ correspond to excitation and relaxation of the two state system. The interaction Hamiltonian describes processes where (i) the two level system in the ground state absorbs a photon from the field and becomes excited, and (ii) the two level system in the excited state emits a photon and relaxes. The parameter γ in the Hamiltonian (2.51) describes the coupling of the field to the two state system. Hamiltonian (2.51) is known as the Jaynes-Cummings Hamiltonian [14–16]. We will derive it in the next section and also discuss the approximations and the coupling constant γ.

2.4.1 Electric-dipole interaction Hamiltonian

The interaction of an atom and a quantized electromagnetic field is given by the term [6,7]

$$\mathcal{H}_{\text{int}} = -\mathbf{d} \cdot \hat{\mathbf{E}}(\mathbf{r}, t), \tag{2.52}$$

where $\mathbf{d} = -e\mathbf{r}_{\text{e}}$ is the electric dipole moment, $\mathbf{r} = \mathbf{r}_0 + \mathbf{r}_{\text{e}}$, where, furthermore, $\mathbf{r}_0$ is the position of the nucleus, and $\mathbf{r}_{\text{e}}$ is the position of the electron relative to the nucleus. Since electron's relative position to nucleus is of the order of Bohr radius $\sim 10^{-11}m$ and the wavevector in visible light regime is of the order of $10^6/m$, the exponential terms in the electric field operator can be approximated as $\exp(\mathrm{i}\mathbf{r}_0 \cdot \mathbf{k} + \mathrm{i}\mathbf{r}_{\text{e}} \cdot \mathbf{k}) \approx \exp(\mathrm{i}\mathbf{r}_0 \cdot \mathbf{k})$. This approximation is known as Dipole approximation. Thus, the Hamiltonian is

$$\mathcal{H}_{\text{int}} = e\mathbf{r} \cdot \hat{\mathbf{E}}(\mathbf{r}_0, t), \tag{2.53}$$

where the single mode electric field operator (see equation. (2.27))

$$\hat{\mathbf{E}}(\mathbf{r}_0, t) = \mathrm{i}\sqrt{\frac{\hbar\omega_{\mathbf{k}}}{2\varepsilon_0 V}}\varepsilon_{\mathbf{k}}\left[\hat{a}_{\mathbf{k}}\exp(-\mathrm{i}\omega_{\mathbf{k}}t + \mathrm{i}\mathbf{k}\cdot\mathbf{r}_0) - \hat{a}_{\mathbf{k}}^\dagger\exp(\mathrm{i}\omega_{\mathbf{k}}t - \mathrm{i}\mathbf{k}\cdot\mathbf{r}_0)\right] \tag{2.54}$$

depends only on the position of the nucleus, not the position of the electron. With the use of the closure theorem ($\sum_{\text{all states}} |i\rangle\langle i| = 1$) the dipole moment can be written as $\mathbf{d} = -e\sum_{i=g}^e |i\rangle\langle i|\mathbf{r}_{\text{e}}\sum_{j=g}^e |j\rangle\langle j| = \sum_{i,j=g}^e \mathbf{d}_{i,j}|i\rangle\langle j|$, where $\mathbf{d}_{i,j} = -e\langle i|\mathbf{r}_{\text{e}}|j\rangle$.

Terms $\langle g|\mathbf{r}_\mathrm{e}|g\rangle = \langle e|\mathbf{r}_\mathrm{e}|e\rangle = 0$ due to the symmetry properties so these terms are dropped. Furthermore, we assume that $\mathbf{d}_{e,g} = \mathbf{d}_{g,e}$ are real vectors. The Hamiltonian can now be written as

$$\mathcal{H}_\mathrm{int} = \hbar\varepsilon_\mathbf{k} \cdot \langle e|\mathbf{r}_\mathrm{e}|g\rangle \left[\gamma_\mathbf{k}\hat{a}_\mathbf{k}\exp(-\mathrm{i}\omega_\mathbf{k}t) + \gamma_\mathbf{k}^*\hat{a}_\mathbf{k}^\dagger\exp(\mathrm{i}\omega_\mathbf{k}t)\right]\left(|e\rangle\langle g| + |g\rangle\langle e|\right), \quad (2.55)$$

where $\gamma_\mathbf{k} = \mathrm{i}\sqrt{\frac{\omega_\mathbf{k}}{2\varepsilon_0\hbar V}}e\exp(\mathrm{i}\mathbf{k}\cdot\mathbf{r}_0)$. Without loss of generality the phase of the polarization vector and the coordinate system can be chosen so that we obtain a real positive coupling constant $\gamma_\mathbf{k}$. We include $\varepsilon_\mathbf{k} \cdot \langle e|\mathbf{r}|g\rangle$ into $\gamma_\mathbf{k}$ and redefine it as

$$\gamma_\mathbf{k} = e\sqrt{\frac{\omega_\mathbf{k}}{2\varepsilon_0\hbar V}}\,|\langle e|\mathbf{r}_\mathrm{e}|g\rangle \cdot \varepsilon_\mathbf{k}\exp(\mathrm{i}\mathbf{k}\cdot\mathbf{r}_0)|\,, \quad (2.56)$$

so that the Hamiltonian is $\mathcal{H}_\mathrm{int} = \hbar\gamma_\mathbf{k}\left[\hat{a}_\mathbf{k}\exp(-\mathrm{i}\omega_\mathbf{k}t) + \hat{a}_\mathbf{k}^\dagger\exp(\mathrm{i}\omega_\mathbf{k}t)\right]\left(|e\rangle\langle g|+|g\rangle\langle e|\right)$. The interaction Hamiltonian is given in a mixed picture. The atomic part is written in the Schrödinger representation while the radiative part is written in the Heisenberg picture. Next we will write the whole system in a single representation. In order to obtain a time independent Hamiltonian we move to the Schrödinger picture i.e. we move the time dependence of the Hamiltonian to the state vector. The Schrödinger equation in the interaction picture gives

$$\left(\mathcal{H}_\mathrm{atom} + \mathcal{H}_\mathrm{int}(t)\right)|\Psi(t)\rangle = \mathrm{i}\hbar\frac{\mathrm{d}}{\mathrm{d}t}|\Psi(t)\rangle, \quad (2.57)$$

where the wavefunction is defined as $|\Psi(t)\rangle = \exp\left(\mathrm{i}\mathcal{H}_\mathrm{field}t/\hbar\right)|\psi(t)\rangle$ giving

$$\left(\mathcal{H}_\mathrm{atom} + \mathcal{H}_\mathrm{int}(t)\right)e^{\mathrm{i}\mathcal{H}_\mathrm{field}t/\hbar}|\psi(t)\rangle = \mathrm{i}\hbar e^{\mathrm{i}\mathcal{H}_\mathrm{field}t/\hbar}\left(\mathrm{i}\frac{\mathcal{H}_\mathrm{field}}{\hbar}|\psi(t)\rangle + \frac{\mathrm{d}}{\mathrm{d}t}|\psi(t)\rangle\right). \quad (2.58)$$

Multiplying from left by $\exp\left(-\mathrm{i}\mathcal{H}_\mathrm{field}t/\hbar\right)$ and using the commutativity of $\mathcal{H}_\mathrm{atom}$ and $\mathcal{H}_\mathrm{field}$ gives

$$\left(\mathcal{H}_\mathrm{field} + \mathcal{H}_\mathrm{atom} + e^{-\mathrm{i}\mathcal{H}_\mathrm{field}t/\hbar}\mathcal{H}_\mathrm{int}(t)e^{\mathrm{i}\mathcal{H}_\mathrm{field}t/\hbar}\right)|\psi(t)\rangle = \mathrm{i}\hbar\frac{\mathrm{d}}{\mathrm{d}t}|\psi(t)\rangle. \quad (2.59)$$

The commutation relations of the annihilation and creation operators give $e^{-\mathrm{i}\omega\hat{a}^\dagger\hat{a}t}\hat{a}e^{\mathrm{i}\omega\hat{a}^\dagger\hat{a}t} = \hat{a}e^{\mathrm{i}\omega t}$ and $e^{-\mathrm{i}\omega\hat{a}^\dagger\hat{a}t}\hat{a}^\dagger e^{\mathrm{i}\omega\hat{a}^\dagger\hat{a}t} = \hat{a}^\dagger e^{-\mathrm{i}\omega t}$. Therefore, the time dependence of $\mathcal{H}_\mathrm{int}(t)$ in equation (2.59) cancels and the electric dipole interaction Hamiltonian in the Schrödinger picture can be written as

$$\mathcal{H}_\mathrm{int} = \hbar\gamma_\mathbf{k}\left(\hat{a}_\mathbf{k} + \hat{a}_\mathbf{k}^\dagger\right)\left(|e\rangle\langle g| + |g\rangle\langle e|\right). \quad (2.60)$$

Finally, we make the rotating wave approximation i.e. drop the terms corresponding to creation of a photon with simultaneous atom excitation and annihilation of a photon with simultaneous atom relaxation and arrive at the Jaynes-Cummings Hamiltonian

$$\mathcal{H}_{\text{int}} = \hbar\gamma_{\mathbf{k}} \left(\hat{a}_{\mathbf{k}}|e\rangle\langle g| + \hat{a}_{\mathbf{k}}^{\dagger}|g\rangle\langle e| \right). \qquad (2.61)$$

2.5 Solution of the Jaynes-Cummings model

We will introduce the analytical and numerical solutions of the well know Jaynes-Cummings model as a background. Later, we will add dissipation and amplification to the standard Jaynes-Cummings model and use similar methods to find solutions of the more complicated system.

2.5.1 Analytical solution

In the Jaynes-Cummings model the system consists of a two state quantum system (atom) and a single mode field. The system is closed and, therefore, energy conserving. Due to the fact that there is no dissipation or amplification, only states $|g, n+1\rangle$ and $|e, n\rangle$ interact with each other. This allows us to find solutions of 2×2 subsystems instead of solving an infinite dimensional system. We will use a method described in [8, 15]. Other approaches are given in [7, 14, 16, 17].

The initial density operator is $\hat{\rho}_{\text{tot}}(0) = \hat{\rho}_{\text{atom}}(0) \otimes \hat{\rho}_{\text{field}}(0)$, where $\hat{\rho}_{\text{field}}$ can be infinite dimensional but we solve the subsystem consisting of the ground state with $n+1$ photons and the excited state with n photons i.e. states $|g, n+1\rangle$ and $|e, n\rangle$. We denote the density operator of the subsystem as $\hat{\rho}_{n+1}$ and the Hamiltonian is written

as

$$\mathcal{H} = \hbar \begin{bmatrix} \omega(\hat{a}^\dagger \hat{a} + 1/2) & \gamma\hat{a} \\ \gamma\hat{a}^\dagger & \omega(\hat{a}^\dagger \hat{a} - 1/2) \end{bmatrix}. \tag{2.62}$$

In this basis the state vectors are $|g\rangle = [0 \quad 1]^{\mathrm{T}}$ and $|e\rangle = [1 \quad 0]^{\mathrm{T}}$. In general the evolution of the density operator is given by [11]

$$\frac{\mathrm{d}\hat{\rho}(t)}{\mathrm{d}t} = -\frac{\mathrm{i}}{\hbar} [\mathcal{H}, \hat{\rho}(t)], \tag{2.63}$$

where $[\mathcal{H}, \hat{\rho}(t)] = \mathcal{H}\hat{\rho}(t) - \hat{\rho}(t)\mathcal{H}$ is the commutator. The formal solution is

$$\hat{\rho}(t) = e^{-\mathrm{i}\mathcal{H}t/\hbar}\hat{\rho}(0)e^{\mathrm{i}\mathcal{H}t/\hbar}, \tag{2.64}$$

as discussed in section 2.2. We will denote unitary evolution operator as $\mathcal{U}(t) = e^{-\mathrm{i}\mathcal{H}t/\hbar}$. First we divide the Hamiltonian into two parts

$$\begin{aligned} \mathcal{H}_1 &= \frac{1}{2}\hbar\omega\sigma_0 + \hbar\omega\hat{a}^\dagger\hat{a} \\ &= \hbar \begin{bmatrix} \omega(\hat{a}^\dagger \hat{a} + 1/2) & 0 \\ 0 & \omega(\hat{a}^\dagger \hat{a} - 1/2) \end{bmatrix} \end{aligned} \tag{2.65}$$

and

$$\begin{aligned} \hat{H}_2 &= \hbar\gamma(\hat{a}\sigma_+ + \hat{a}^\dagger\sigma_-) \\ &= \hbar \begin{bmatrix} 0 & \gamma\hat{a} \\ \gamma\hat{a}^\dagger & 0 \end{bmatrix}. \end{aligned} \tag{2.66}$$

The unitary evolution operators are $\mathcal{U}_i(t) = \exp(-\mathrm{i}\mathcal{H}_i t/\hbar)$ giving

$$\mathcal{U}_1 = \begin{bmatrix} e^{-\mathrm{i}\omega(\hat{a}^\dagger\hat{a}+1/2)t} & 0 \\ 0 & e^{-\mathrm{i}\omega(\hat{a}^\dagger\hat{a}-1/2)t} \end{bmatrix} \tag{2.67}$$

and

$$\mathcal{U}_2 = \sum_{k=0}^{\infty} \frac{(-\mathrm{i})^k t^k}{k!} \begin{bmatrix} 0 & \gamma\hat{a} \\ \gamma\hat{a}^\dagger & 0 \end{bmatrix}^k. \tag{2.68}$$

$$= \begin{bmatrix} \cos(\gamma\sqrt{\hat{n}+1}t) & -\mathrm{i}\frac{\sin(\gamma\sqrt{\hat{n}+1}t)}{\sqrt{\hat{n}+1}}\hat{a} \\ -\mathrm{i}\hat{a}^\dagger\frac{\sin(\gamma\sqrt{\hat{n}+1}t)}{\sqrt{\hat{n}+1}} & \cos(\gamma\sqrt{\hat{n}}t) \end{bmatrix}. \tag{2.69}$$

Assuming that the system's initial state is $\hat{\rho}(0) = |g\rangle\langle g| \otimes \hat{\rho}_{\text{field}}$ and substituting $\mathcal{U}(t) = \mathcal{U}_1(t)\mathcal{U}_2(t)$ into equation (2.64) gives the elements of subsystem $\hat{\rho}_{n+1}$ as $p_{g,n} = \cos^2\left(\gamma\sqrt{n}t\right)p_n(0)$ and $p_{e,n} = \sin^2\left(\gamma\sqrt{n+1}t\right)p_{n+1}(0)$. Therefore, the ground state, the excited state, and the n photon state probabilities are obtained as sums

$$p_g(t) = \sum_{n=0}^{\infty}\cos^2\left(\gamma t\sqrt{n}\right)p_n(0) \tag{2.70}$$

$$p_e(t) = \sum_{n=0}^{\infty}\sin^2\left(\gamma t\sqrt{n+1}\right)p_{n+1}(0) \tag{2.71}$$

$$p_n(t) = p_{g,n}(t) + p_{e,n}(t). \tag{2.72}$$

2.5.2 Numerical solution

The numerical solution of the subsystems $\hat{\rho}_{n+1}$ can be found applying equation (2.63). For a small time step Δt we can write $\hat{\rho}_{n+1}(t + \Delta t) = \hat{\rho}_{n+1}(t) + (-\mathrm{i}\Delta t/\hbar)[\mathcal{H}, \hat{\rho}_{n+1}(t)]$. Substitution of Hamiltonian (2.62) gives

$$\hat{\rho}_{n+1}(\tau + \Delta\tau) = \hat{\rho}_{n+1}(\tau)$$
$$+\Delta\tau\begin{bmatrix} -\mathrm{i}\sqrt{n+1}(\rho_{ge}^{n+1}(\tau) - \rho_{eg}^{n+1}(\tau)) & -\mathrm{i}\sqrt{n+1}(\rho_{gg}^{n+1}(\tau) - \rho_{ee}^{n+1}(\tau)) \\ -\mathrm{i}\sqrt{n+1}(\rho_{ee}^{n+1}(\tau) - \rho_{gg}^{n+1}(\tau)) & -\mathrm{i}\sqrt{n+1}(\rho_{eg}^{n+1}(\tau) - \rho_{ge}^{n+1}(\tau)) \end{bmatrix},$$
$$\tag{2.73}$$

where we have scaled the time with the coupling parameter as $\tau = \gamma t$ to obtain results independent of the coupling constant.

2.5.3 Rabi oscillations

The repeated absorption and emission of a photon by a two state system is called the Rabi oscillation [6–8, 10] which can be modeled using the Jaynes-Cummings model. Example solutions of the Jaynes-Cummings model are given in figure 2.1. The two state system is initially in the ground state and the initial field state is (a) the single

photon Fock state, and (b) the thermal field with $\bar{n}(0) = 1$. In case (a) clear repeated absorption and emission (Rabi oscillations) are seen while in case (b) oscillation is a mixture of different oscillation frequencies due to the more complicated initial field state.
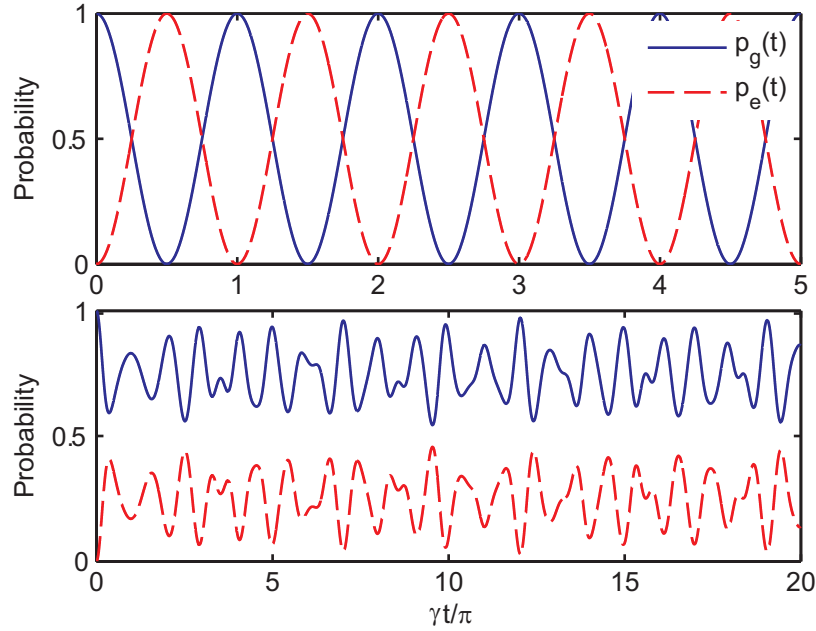
Figure 2.1: Solution of the Jaynes-Cummings model having the two state system initially in the ground state and field in (a) single photon Fock state $|1\rangle$ (b) thermal field with $\bar{n}(0) = 1$. The atom oscillates between the excited state and the ground state. It emits and absorbs a single photon repeatedly. This phenomenon is called Rabi oscillation.

2.6   Quantum correlation and coherence

Correlation of photons in a field can be used to discriminate the statistical properties of the field. Correlation function is also a crucial component of the coincidence photodetection theory. First we define the correlation functions and coherence degree functions and then we calculate the coherence degrees for common optical fields. Correlation functions will be later applied to derive the coincidence detection prob-

abilities (publication I). The second order coherence degree is used to analyze the produced optical fields (publications I, IV and VI).

The nth order correlation function and the nth order coherence degree of the quantized field are, respectively, given by [2, 3, 6, 17]

$$
\begin{aligned}
G^{(n)}(\mathbf{r}_1, t_1, \mathbf{r}_2, t_2, \ldots, \mathbf{r}_{2n}, t_{2n}) &= \text{Tr}\{\hat{\rho}\hat{\mathbf{E}}^{(-)}(\mathbf{r}_1, t_1) \ldots \hat{\mathbf{E}}^{(-)}(\mathbf{r}_n, t_n) \\
&\qquad \hat{\mathbf{E}}^{(+)}(\mathbf{r}_{n+1}, t_{n+1}) \ldots \hat{\mathbf{E}}^{(+)}(\mathbf{r}_{2n}, t_{2n})\}
\end{aligned}
\tag{2.74}
$$

$$
g^{(n)}(\mathbf{r}_1, t_1, \mathbf{r}_2, t_2, \ldots \mathbf{r}_n, t_n) = \frac{G^{(n)}(\mathbf{r}_1, t_1, \ldots, \mathbf{r}_n, t_n, \mathbf{r}_n, t_n, \ldots, \mathbf{r}_1, t_1)}{G^{(1)}(\mathbf{r}_1, t_1, \mathbf{r}_1, t_1) \ldots G^{(n)}(\mathbf{r}_n, t_n, \mathbf{r}_n, t_n)}.
\tag{2.75}
$$

In the correlation functions a scalar products of the electric field operator vectors are taken.

A special case of coherence degrees for quantum fields is the second order coherence degree $g^{(2)}(\mathbf{r}_1, t_1, \mathbf{r}_2, t_2) = \text{Tr}\{\hat{\rho}\hat{a}^\dagger\hat{a}^\dagger\hat{a}\hat{a}\}/\text{Tr}\{\hat{\rho}\hat{a}^\dagger\hat{a}\}^2$ of the single mode optical fields giving

$$
g^{(2)}(\mathbf{r}_1, t_1, \mathbf{r}_2, t_2) = \frac{\overline{n(n-1)(0)}}{\bar{n}^2(0)},
\tag{2.76}
$$

where $\bar{n}(0)$ is the number of photons in the initial field and $\overline{n(n-1)(0)}$ is the second factorial moment of the initial field. The second order coherence degree is an important measure of photon correlation in photon detection experiments describing the photon bunching and anti-bunching phenomena as follows [6]

$$
g^{(2)}(0) > 1 \qquad \text{bunched light} \tag{2.77}
$$

$$
g^{(2)}(0) = 1 \qquad \text{Poissonian light} \tag{2.78}
$$

$$
0 \leq g^{(2)}(0) < 1 \qquad \text{anti-bunched light} \tag{2.79}
$$

where $g^{(2)}(0) = g^{(2)}(\mathbf{r}, 0, \mathbf{r}, 0)$. The second order coherence degrees for the single mode Fock state, coherent field and thermal field are $g_{\text{Fock}}^{(2)}(0) = (N - 1)/N$ ($|N\rangle$ is the initial state), $g_{\text{coh}}^{(2)}(0) = 1$, and $g_{\text{ther}}^{(2)}(0) = 2$, as will be shown below. Thus, these fields are examples of anti-bunched, non-bunched and bunched lights.

Other measures of the correlation are also used. For example, Mandel's Q parameter is defined as [18]

$$Q = \frac{\overline{n(n-1)} - \bar{n}^2}{\bar{n}} = \bar{n}\left(g^{(2)}(0) - 1\right). \tag{2.80}$$

Furthermore, a normalized version of the Mandel's parameter as a more appropriate measure in experimental use, has been proposed as [19]

$$Q_{\text{norm}} = \frac{Q}{\bar{n}} = g^{(2)}(0) - 1. \tag{2.81}$$

2.6.1 Coherence degrees of Fock states

The first and second order correlations of a single mode Fock state $|N_{\mathbf{k}}\rangle$ are

$$G^{(1)}(\mathbf{r}_1, t_1, \mathbf{r}_2, t_2) = \frac{\hbar}{2\varepsilon_0 V}\omega_{\mathbf{k}} N_{\mathbf{k}} e^{-i\mathbf{k}\cdot(\mathbf{r}_1-\mathbf{r}_2)+i\omega_{\mathbf{k}}(t_1-t_2)} \tag{2.82}$$

$$G^{(2)}(\mathbf{r}_1, t_1, \mathbf{r}_2, t_2) = \frac{\hbar^2}{(2\varepsilon_0 V)^2}\omega_{\mathbf{k}}^2 N_{\mathbf{k}}(N_{\mathbf{k}} - 1), \tag{2.83}$$

and the first order and the second order coherence degrees are

$$\begin{aligned}
g^{(1)}(\mathbf{r}_1, t_1, \mathbf{r}_2, t_2) &= \frac{G^{(1)}(\mathbf{r}_1, t_1, \mathbf{r}_2, t_2)}{\sqrt{G^{(1)}(\mathbf{r}_1, t_1, \mathbf{r}_1, t_1)G^{(1)}(\mathbf{r}_2, t_2, \mathbf{r}_2, t_2)}} \\
&= e^{-i\mathbf{k}\cdot(\mathbf{r}_1-\mathbf{r}_2)+i\omega_{\mathbf{k}}(t_1-t_2)} \tag{2.84} \\
g^{(2)}(\mathbf{r}_1, t_1, \mathbf{r}_2, t_2) &= \frac{G^{(2)}(\mathbf{r}_1, t_1, \mathbf{r}_2, t_2)}{G^{(1)}(\mathbf{r}_1, t_1, \mathbf{r}_1, t_1)G^{(1)}(\mathbf{r}_2, t_2, \mathbf{r}_2, t_2)} \\
&= \frac{(N_{\mathbf{k}} - 1)}{N_{\mathbf{k}}}. \tag{2.85}
\end{aligned}$$

2.6.2 Coherence degrees of thermal fields

It can be shown that the first and second order correlations of the thermal field are

$$\begin{aligned}
G^{(1)}(\mathbf{r}_1, t_1, \mathbf{r}_2, t_2) &= \frac{\hbar}{2\varepsilon_0 V}\sum_{\mathbf{k}}\omega_{\mathbf{k}}\bar{n}_{\mathbf{k}} e^{-i\mathbf{k}\cdot(\mathbf{r}_1-\mathbf{r}_2)+i\omega_{\mathbf{k}}(t_1-t_2)} \tag{2.86} \\
G^{(2)}(\mathbf{r}_1, t_1, \mathbf{r}_2, t_2) &= G^{(1)}(\mathbf{r}_1, t_1, \mathbf{r}_1, t_1)G^{(1)}(\mathbf{r}_2, t_2, \mathbf{r}_2, t_2) \\
&\quad + G^{(1)}(\mathbf{r}_1, t_1, \mathbf{r}_2, t_2)G^{(1)}(\mathbf{r}_2, t_2, \mathbf{r}_1, t_1) \tag{2.87}
\end{aligned}$$

Furthermore, the first order and the second order coherence degrees are

$$g^{(1)}(\mathbf{r}_1, t_1, \mathbf{r}_2, t_2) = \frac{\sum_{\mathbf{k}} \omega_{\mathbf{k}} \overline{n}_{\mathbf{k}} e^{-i\mathbf{k}\cdot(\mathbf{r}_1 - \mathbf{r}_2) + i\omega_{\mathbf{k}}(t_1 - t_2)}}{\sum_{\mathbf{k}} \omega_{\mathbf{k}} \overline{n}_{\mathbf{k}}} \tag{2.88}$$

$$g^{(2)}(\mathbf{r}_1, t_1, \mathbf{r}_2, t_2) = \frac{G^{(2)}(\mathbf{r}_1, t_1, \mathbf{r}_2, t_2)}{G^{(1)}(\mathbf{r}_1, t_1, \mathbf{r}_1, t_1) G^{(1)}(\mathbf{r}_2, t_2, \mathbf{r}_2, t_2)}$$

$$= 1 + \left| g^{(1)}(\mathbf{r}_1, t_1, \mathbf{r}_2, t_2) \right|^2. \tag{2.89}$$

The nth order correlation function for the thermal field can be written as a sum of products of n first order correlation functions. The sum is taken over all possible permutations of n points so there is $n!$ terms. The nth order correlation is

$$G^{(n)}(\mathbf{r}_1, t_1, \ldots, \mathbf{r}_n, t_n, \mathbf{r}_n, t_n \ldots, \mathbf{r}_1, t_1)$$

$$= \sum_{\substack{\text{permut.} \\ \text{of } y}} \prod_{l=1}^{n} G^{(1)}(\mathbf{r}_l, t_l, \mathbf{r}_{y(l)}, t_{y(l)}), \tag{2.90}$$

where the sum is taken over all the possible permutations of indexes $y = [1, 2, \ldots, n]$. Thus the nth order coherence degree is

$$g^{(n)}(\mathbf{r}_1, t_1, \ldots, \mathbf{r}_n, t_n) = \frac{\sum_{\substack{\text{permut.} \\ \text{of } y}} \prod_{l=1}^{n} G^{(1)}(\mathbf{r}_l, t_l, \mathbf{r}_{y(l)}, t_{y(l)})}{\prod_{l=1}^{n} G^{(1)}(\mathbf{r}_l, t_l, \mathbf{r}_l, t_l)} \tag{2.91}$$

and $g^{(n)}(\mathbf{r}, t, \ldots, \mathbf{r}, t) = n!$

2.6.3   Coherence degrees of coherent fields

For the coherent field the first and second order correlations can be shown to be

$$G^{(1)}(\mathbf{r}_1, t_1, \mathbf{r}_2, t_2) = \frac{\hbar}{2\varepsilon_0 V} \left(\sum_{\mathbf{k}} \sqrt{\omega_{\mathbf{k}}} \alpha_{\mathbf{k}}^* e^{-i\mathbf{k}\cdot\mathbf{r}_1 + i\omega_{\mathbf{k}} t_1} \right) \tag{2.92}$$

$$\times \left(\sum_{\mathbf{k}} \sqrt{\omega_{\mathbf{k}}} \alpha_{\mathbf{k}} e^{+i\mathbf{k}\cdot\mathbf{r}_2 - i\omega_{\mathbf{k}} t_2} \right)$$

$$G^{(2)}(\mathbf{r}_1, t_1, \mathbf{r}_2, t_2) = G^{(1)}(\mathbf{r}_1, t_1, \mathbf{r}_1, t_1) G^{(1)}(\mathbf{r}_2, t_2, \mathbf{r}_2, t_2). \tag{2.93}$$

Furthermore, the nth order correlation of the coherent field can be written as a product of the first order correlation terms

$$G^{(n)}(\mathbf{r}_1, t_1, \ldots, \mathbf{r}_n, t_n, \mathbf{r}_n, t_n \ldots, \mathbf{r}_1, t_1) = \prod_{l=1}^{n} G^{(1)}(\mathbf{r}_l, t_l, \mathbf{r}_l, t_l). \tag{2.94}$$

The coherence degrees are given by

$$
g^{(1)}(\mathbf{r}_1, t_1, \mathbf{r}_2, t_2) = \frac{\sum_{\mathbf{k}} \sqrt{\omega_{\mathbf{k}}} \alpha_{\mathbf{k}}^* e^{-i\mathbf{k}\cdot\mathbf{r}_1 + i\omega_{\mathbf{k}} t_1}}{\left|\sum_{\mathbf{k}} \sqrt{\omega_{\mathbf{k}}} \alpha_{\mathbf{k}}^* e^{-i\mathbf{k}\cdot\mathbf{r}_1 + i\omega_{\mathbf{k}} t_1}\right|} \frac{\sum_{\mathbf{k}} \sqrt{\omega_{\mathbf{k}}} \alpha_{\mathbf{k}} e^{+i\mathbf{k}\cdot\mathbf{r}_2 - i\omega_{\mathbf{k}} t_2}}{\left|\sum_{\mathbf{k}} \sqrt{\omega_{\mathbf{k}}} \alpha_{\mathbf{k}} e^{+i\mathbf{k}\cdot\mathbf{r}_2 - i\omega_{\mathbf{k}} t_2}\right|} \quad (2.95)
$$

$$
g^{(2)}(\mathbf{r}_1, t_1, \mathbf{r}_2, t_2) = \frac{G^{(2)}(\mathbf{r}_1, t_1, \mathbf{r}_2, t_2)}{G^{(1)}(\mathbf{r}_1, t_1, \mathbf{r}_1, t_1) G^{(1)}(\mathbf{r}_2, t_2, \mathbf{r}_2, t_2)} = 1. \quad (2.96)
$$

For coherent field the nth order coherence degree is given by

$$
g^{(n)}(\mathbf{r}_1, t_1, \ldots, \mathbf{r}_n, t_n) = \frac{\prod_{l=1}^{n} G^{(1)}(\mathbf{r}_l, t_l, \mathbf{r}_l, t_l)}{\prod_{l=1}^{n} G^{(1)}(\mathbf{r}_l, t_l, \mathbf{r}_l, t_l)} = 1. \quad (2.97)
$$

Thus, the coherence degree $g^{(n)}$ of a coherent field is always one for $n > 1$ and $|g^{(1)}(\mathbf{r}_1, t_1, \mathbf{r}_2, t_2)| = 1$.

3 Open quantum systems: dissipation and amplification

We have considered in all our publications (I–VI) open quantum systems including dissipation of energy and/or energy injection. In closed quantum systems the dynamics is described by a unitary time evolution operator as discussed in section 2.2. The dynamics of open quantum systems cannot in general be described by a unitary time evolution. Instead a master equation approach needs to be used. We will define a first order linear differential equation for the density operator called Markovian master equation of Lindblad form. Depending on the interactions of the system with the environment the Lindblad master equation can model dissipation, amplification, or both. In this thesis we consider Markovian processes which means that the equations of motion of system $\hat{\rho}(t)$ at time t depend only on the system's current state $\hat{\rho}(t)$, not on the previous states.

3.1 Lindblad master equation and quantum jump superoperators

The dynamics of an open system $\hat{\rho}(t)$ is governed by the Lindblad master equation [11, 12, 20–24]

$$\frac{\mathrm{d}\hat{\rho}(t)}{\mathrm{d}t} = -\frac{\mathrm{i}}{\hbar} \left[\mathcal{H}_0, \hat{\rho}(t) \right] - \sum_l \frac{\gamma_l}{2} \left(\hat{L}_l^\dagger \hat{L}_l \hat{\rho}(t) - 2\hat{L}_l \hat{\rho}(t) \hat{L}_l^\dagger + \hat{\rho}(t) \hat{L}_l^\dagger \hat{L}_l \right), \qquad (3.1)$$

where $\mathcal{H}_0$ is the Hamiltonian operator of reversible dynamics, and γ_l is the rate of the irreversible process l described by operator $\hat{L}_l$. These irreversible processes are for example a photon subtraction and a photon addition from/to the system and e.g. for the damped harmonic oscillator $\hat{L} = \hat{a}$. Operator $\hat{J}\hat{\rho} = \gamma_l \hat{L}_l \hat{\rho} \hat{L}_l^\dagger$ models a quantum jump and is called quantum jump superoperator (QJS).

3.1.1 Quantum trajectories

For simplicity we consider a system described by equation (3.1) with one jump mechanism (or jump channel) so that $l = 1$. During an infinitesimal time interval $[t, t + \mathrm{d}t)$ the evolution of the system is given by

$$\hat{\rho}(t + \mathrm{d}t) = \hat{S}\hat{\rho}(t)\mathrm{d}t + \hat{J}\hat{\rho}(t)\mathrm{d}t, \tag{3.2}$$

where the jump event is described by QJS $\hat{J}$ and the rest of the terms in equation (3.1) are governed by the no-jump superoperator $\hat{S}$. If it is possible to detect the jump, the state of the system collapses into a state defined by the QJS i.e. the new state is $\hat{J}\hat{\rho}(t)/\mathrm{Tr}\{\hat{J}\hat{\rho}(t)\}$. Similarly, if it is detected that there is no jump event, the new state is given by $\hat{S}\hat{\rho}(t)/\mathrm{Tr}\{\hat{S}\hat{\rho}(t)\}$. The probabilities of the jump event and the no-jump event are, respectively, given by

$$p_{\mathrm{jump}} = \mathrm{Tr}\{\hat{J}\hat{\rho}(t)\}\mathrm{d}t \tag{3.3}$$

$$p_{\mathrm{no-jump}} = \mathrm{Tr}\{\hat{S}\hat{\rho}(t)\}\mathrm{d}t. \tag{3.4}$$

The time interval $[t, t + \mathrm{d}t)$ in equation (3.2) must be so short that at most one jump event can occur i.e. $p_{\mathrm{jump}} + p_{\mathrm{no-jump}} = 1$. If no jumps are detected during a non-infinitesimal time interval $[t, t + t_1)$ the no-jump superoperator can be solved from equation (3.1) giving

$$\hat{S}(t_1)\hat{\rho}(t) = e^{-i\mathcal{H}_0 t_1/\hbar - \gamma \hat{L}^\dagger \hat{L} t_1/2}\hat{\rho}(t)e^{+i\mathcal{H}_0 t_1/\hbar - \gamma \hat{L}^\dagger \hat{L} t_1/2}. \tag{3.5}$$

The Lindblad master equation (3.1) gives the average evolution of the system. In contrast, operators $\hat{J}$ and $\hat{S}$ give certain trajectories as a result of the system collapsing to states defined by the measurement outcomes. The average of the trajectories of an ensemble of systems reproduces the dynamics given by the Lindblad master equation.

Also more complicated trajectories can be described by using the jump and no-jump operators. For example, $\mathrm{Tr}\{\hat{J}\hat{S}(t)\hat{\rho}(0)\mathrm{d}t\}$ is the probability that the first

jump occurs during $[t, t + \mathrm{d}t)$, whereas the relation

$$\hat{\rho}(t) = \frac{\int_{t_1=0}^{t} \hat{S}(t - t_1) \hat{J} \hat{S}(t_1) \hat{\rho}(0) \mathrm{d}t_1}{\mathrm{Tr}\{\int_{t_1=0}^{t} \hat{S}(t - t_1) \hat{J} \hat{S}(t_1) \hat{\rho}(0) \mathrm{d}t_1\}} \tag{3.6}$$

corresponds to a trajectory where one and only one jump event have occurred during $[0, t)$.

4 Optical devices and experimental setups

Many fundamental experiments analyzed in this thesis can be performed with relatively simple, but high quality optical instruments like light sources, beam splitters and detectors. This, however, requires careful planning of the experiments, detailed analysis of the results, and good understanding of the setup and the quantum optical properties of the fields and the instruments. In this section we give a short introduction to the elementary components and define their impact on the fields within the quantum trajectory approach.
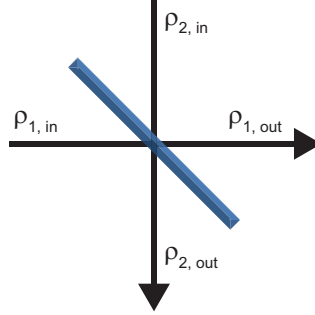
4.1 Beam splitters

A beam splitter (BS) is a passive device which divides an incoming beam by partly passing it through and partly reflecting it. Schematic picture of a beam splitter is shown in figure 4.1. A simple realization of a BS is a partly reflecting mirror. The output field of a BS is given by [4, 20, 25–29]

$$\hat{\rho}_{\text{out}} = \hat{B}\hat{\rho}_{\text{in}}\hat{B}^{\dagger}, \tag{4.1}$$

where $\hat{B} = \exp\left(\theta(\hat{a}_1^{\dagger}\hat{a}_2 - \hat{a}_1\hat{a}_2^{\dagger})\right)$ and it is assumed that BS causes zero phase shift, θ gives the transmission and reflection probabilities as $T = \cos^2(\theta)$ and $R = \sin^2(\theta)$, $\hat{\rho}_{\text{in}} = \hat{\rho}_{\text{in},1} \otimes \hat{\rho}_{\text{in},2}$, and $\hat{a}_i$ operates on mode i. In many experiments [4,30] a conditional output field is obtained by measuring one of the two outputs of the BS. Then the output field is obtained from equation (4.1) by collapsing the measured output mode into the measured state and normalizing. For example in the single photon subtraction experiments (an arbitrary initial field in input mode 1 and a vacuum field in input mode 2) one photon is measured from the output mode 2 giving the

following density operator for the output mode 1

$$\hat{\rho}_{\text{out},1} = \frac{\langle 1_{\text{out},2}|\hat{B}\hat{\rho}_{\text{in},1} \otimes |0_{\text{in},2}\rangle\langle 0_{\text{in},2}|\hat{B}^{\dagger}|1_{\text{out},2}\rangle}{\text{Tr}\left\{\langle 1_{\text{out},2}|\hat{B}\hat{\rho}_{\text{in},1} \otimes |0_{\text{in},2}\rangle\langle 0_{\text{in},2}|\hat{B}^{\dagger}|1_{\text{out},2}\rangle\right\}}. \tag{4.2}$$

Figure 4.1: A beam splitter has two input modes ($\hat{\rho}_{1,\text{in}}$ and $\hat{\rho}_{2,\text{in}}$) and two output modes ($\hat{\rho}_{1,\text{out}}$ and $\hat{\rho}_{2,\text{out}}$). Depending on the transmission coefficient T and the reflection coefficient R of the beam splitter, part of the input mode 1 (2) is transmitted to output mode 1 (2) and reflected to output mode 2 (1).

4.2 Detectors

4.2.1 Photomultiplier tube

The photomultiplier tube (PMT) is based on the photoelectric effect, in which the energy of the incident photon exceeds the work function of the photocathode material allowing an electron to escape from the photocathode. In addition to the photocathode, PMTs consist of dynodes and an anode in a vacuum tube, see figure 4.2.

The PMT operates as follows: The photocathode emits an electron as a consequence of an incident photon and the photoelectric effect. The electron strikes to the first dynode which is biased to a positive voltage. The collision releases more electrons.

The second dynode is biased at a higher voltage than the first one so that the emitted electrons are again accelerated to release more electrons. Each dynode is biased at a higher voltage than the previous one. Finally, a macroscopic charge ($10^4 - 10^7$ electrons [31, 32]) reaches the anode and causes a current pulse. PMTs can detect single photons and resolve the photon number [31]. They have been used since 1930s [33] and are still used in recent experiments [19].
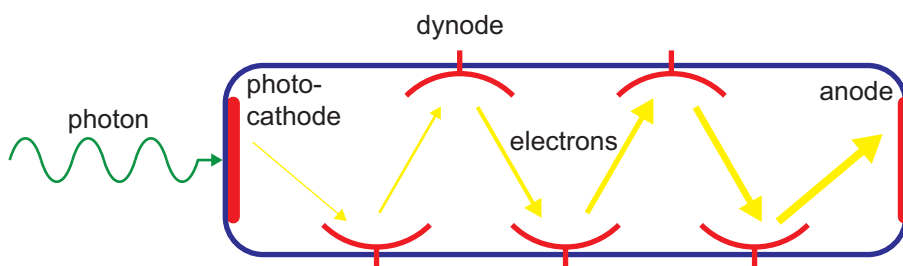
Figure 4.2: A photomultiplier tube consists of photocathode, dynodes, and anode in a vacuum enclosed in a glass tube. A photon releases an electron from the photocathode due to the photoelectric effect. Dynodes are held at increasing voltages so that the electrons accelerate and release more electrons at each dynode. Finally, the charges arrive at the anode and create a current pulse.

4.2.2 Avalanche photodiode

Avalanche photodiode (APD) is a semiconductor photodiode operated at a high reverse bias voltage. The absorption of a photon generates an electron-hole pair. Due to the high bias voltage the carriers are accelerated and the electron or the hole can generate another electron-hole pair by collision. Repetition of this avalanche effect significantly amplifies the photocurrent. APDs are capable to detect single photons but are usually not able to resolve the photon number [31]. Several recent experiments have been performed using APDs [4, 34–39].
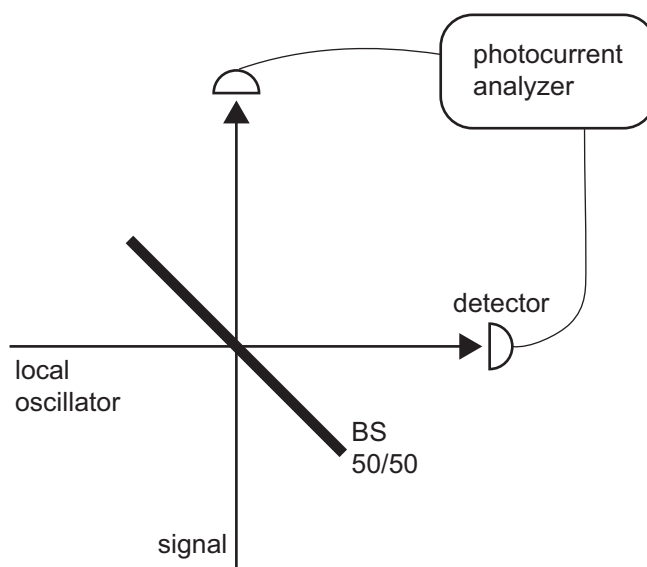
4.2.3 Balanced homodyne detection scheme

In balanced homodyne detection a low intensity signal interferes with a high intensity laser signal (called local oscillator) in a 50/50 ($T = R = 50\%$) beam splitter [27, 40, 41], see figure 4.3. The frequency of the laser is equal to the input signal and it provides a reference signal to the measurement. Let annihilation operator $\hat{a}$ operate on the incoming signal mode and $\hat{a}_{LO}$ on the incoming local oscillator (LO) mode. Then the output modes of the BS are described by $\hat{a}_1 = (\hat{a} + \hat{a}_{LO})/\sqrt{2}$ and $\hat{a}_2 = (\hat{a} - \hat{a}_{LO})/\sqrt{2}$, and therefore, the difference in the photon numbers of the output modes is $\hat{n}_{1-2} = \hat{n}_1 - \hat{n}_2 = \hat{a}^\dagger \hat{a}_{LO} + \hat{a}_{LO}^\dagger \hat{a}$. Similarly the sum of the photon numbers is $\hat{n}_{1+2} = \hat{a}^\dagger \hat{a} + \hat{a}_{LO}^\dagger \hat{a}_{LO}$. The local oscillator is assumed to be a high intensity coherent signal giving the photon number difference and sum as [40, 41]

$$\hat{n}_{1-2} = |\alpha| \left(\hat{a}^\dagger e^{\mathrm{i}\phi} + \hat{a} e^{-\mathrm{i}\phi} \right) \tag{4.3}$$

$$\hat{n}_{1+2} = |\alpha|^2 + \hat{a}^\dagger \hat{a} \approx |\alpha|^2, \tag{4.4}$$

where $|\alpha|$ is the amplitude of the oscillator signal and ϕ is the phase difference between the signal and the local oscillator. With the use of the quadrature variables $\hat{q} = (\hat{a} + \hat{a}^\dagger)/\sqrt{2}$ and $\hat{p} = \mathrm{i}(\hat{a}^\dagger - \hat{a})/\sqrt{2}$ (with $[\hat{q}, \hat{p}] = \mathrm{i}$) the photocurrent difference can be shown to be proportional to a rotated quadrature $\hat{q}_\phi = \hat{q}\cos(\phi) + \hat{p}\sin(\phi)$. Measuring $\hat{q}_\phi$ of equally prepared states for varying ϕ gives the probability distribution of $\hat{q}_\phi$. The normalization of the signal is obtained by measuring the sum of the photocurrents $\hat{n}_{1+2}$.

Using the balanced homodyne detection Wigner's quasi-probability function of the input signal can be reproduced [27, 38–43]. From the measured Wigner function properties like photon number or density operator of the light field can be calculated [10, 20, 40]. Balanced homodyne detection is widely used in recent experiments [38, 40, 42, 43] This kind of quantum state reconstruction is called quantum tomography.

Figure 4.3: Schematic picture of balanced homodyne detection. An input signal interferences with high intensity coherent signal (local oscillator) in a 50/50 beam splitter (BS). The photocurrents are analyzed to reproduce the input signal.

4.2.4   Atom beam detection scheme

Cavity fields can be produced and manipulated with a beam of atoms resonant with the cavity, see figure 4.4. The atoms are initially prepared to a certain state and after passing through the cavity the states of the atoms are measured. The measurement of the atom collapses the cavity field to a corresponding state [44–48]. For example, detection of photons in cavity can be performed by preparing the atoms into the ground state, passing them through the cavity, and measuring the state of atom. If the measured atom is in the excited state a single photon is absorbed. This kind of setup has been theoretically analyzed [49] and experimentally implemented [44]. Similar setups have been used also to create arbitrary Fock states [47] and for quantum non-demolition measurements, where the number of photons is measured without absorbing them [45, 46, 48].
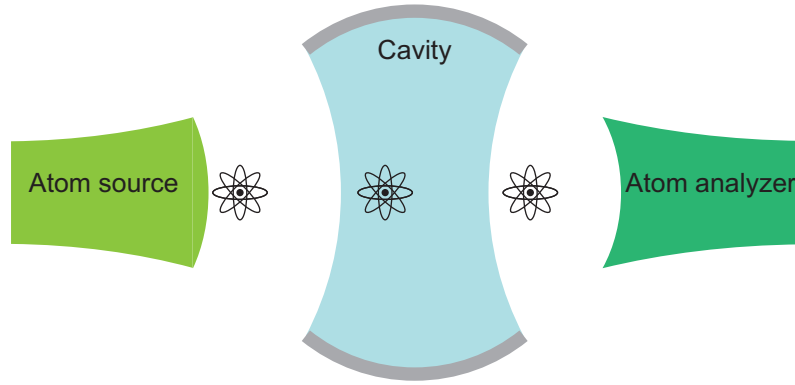
Figure 4.4: Atom beam detection scheme. Atoms prepared to a certain initial state pass through the cavity one at the time. The states of the atoms are measured after the cavity so that the state of the cavity field collapses according to the measurement.

4.3 Light emitting devices

In the following a short introduction to the principles of light emitting diodes and lasers is given. The purpose is not to give a detailed mathematical description but instead explain the basic operation of the devices since we will later apply our model to describe the operation of light emitting diodes and lasers.

In semiconductors the carriers occupy the energy bands according to the Fermi-Dirac distribution in equilibrium. In non-equilibrium, caused for example by carrier injection, the electron occupation probability in the conduction band and the hole occupation probability in the valence band are given by [50, 51]

$$f_e(E) = \left(1 + \exp\left(\frac{E - E_{F,e}}{k_B T}\right)\right)^{-1} \tag{4.5}$$

$$f_h(E) = \left(1 + \exp\left(\frac{E_{F,h} - E}{k_B T}\right)\right)^{-1}, \tag{4.6}$$

where $E_{F,e}$ is the quasi-Fermi level of electrons, $E_{F,h}$ is the quasi-Fermi level of holes, T is the temperature, and k_B is the Boltzmann's constant, see figure 4.5. The absorption rate r_{abs} of photons is proportional to the probabilities of having an

empty state in the conduction band and an electron in the valence band so that

$$r_{\text{abs}} = W(1 - f_e(E_C))(1 - f_h(E_V))\bar{n}, \tag{4.7}$$

where we have assumed that transition occurs between an electron state with $E = E_C$ and a hole state with $E = E_V$. W is a material dependent constant of the carrier, and $\bar{n}$ is the mean number of photons. The emission rate is

$$r_{\text{em}} = W f_e(E_C) f_h(E_V)(\bar{n} + 1), \tag{4.8}$$

where the part depending on $\bar{n}$ corresponds to stimulated emission while the part independent of $\bar{n}$ corresponds to spontaneous emission. To produce optical gain the stimulated emission rate has to be greater than the absorption rate giving the following condition

$$f_e(E_C) + f_h(E_V) > 1. \tag{4.9}$$
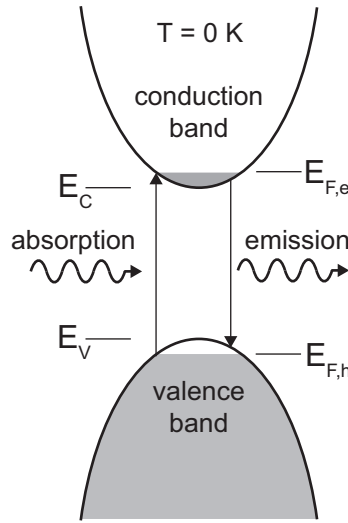
Figure 4.5: Schematic diagram of absorption and emission in semiconductors.

4.3.1 Light emitting diode

Light emitting diode (LED) is a component which emits photons due to the spontaneous emission. Its operation is based on a pn-junction, where p-type and n-type

semiconductors are joint. The p-type semiconductor is a semiconductor material doped with atoms that act as acceptors i.e. take electrons from the valence band of the semiconductor and thereby increase the hole population. In contrast, n-type materials are doped with atoms that act as donors releasing extra electrons to the conduction band of the semiconductor. If the pn-junction is forward biased (positive voltage is applied on the p-side) electrons are injected into the n-side and holes into the p-side. This creates imbalance which results in the onset of various relaxation processes like spontaneous emission producing light output. The statistics of the light field created by an LED corresponds to the statistics of a thermal field.

Although the implemented LEDs are mainly pn-junction based semiconductor devices, in this thesis, setups that operate below the laser threshold producing thermal fields, are considered to operate as LEDs.

4.3.2 Laser

Laser (Light amplification by stimulated emission of radiation) produces a coherent light field by stimulated emission. Semiconductor lasers are also based on the pn-junction. In this case p-type and n-type materials are usually heavily doped and the current injected to the pn-junction is higher than in the LED to reach population inversion i.e. to have more electrons in the higher energy state (close to the edge of the conduction band) than in the lower energy state (close to the edge of the valence band). An essential part of the laser is an optical cavity which consists of highly reflective walls. The light is emitted into the standing waves inside the cavity (into the cavity modes). Due to the population inversion the photons in the cavity more likely stimulate the emission of an additional photon than are absorbed. As a consequence the intensity of the light is increased coherently until the injected energy is not able to maintain the population inversion and the gain saturates.

There are also other types of lasers than the semiconductor laser. For example in the gas laser atoms inside a cavity are optically pumped so that population inversion occurs between the states involved in the emission process.

5   Photon counting statistics

We will consider cavity photon counting and also detection of photons from a light field incident on a beam splitter. The resolving and non-resolving detector schemes are derived and applied to coincidence photon detection in publication I. In publications II and V these schemes are applied to investigate the dynamics of single photon subtracted and added fields.

5.1   Resolving and non-resolving detector models

In the first quantum photodetection theories the optical field was considered to propagate to the detector in open space [2, 52]. Later the optical field was considered to be confined in a cavity with a detector inside the cavity or with a detector absorbing all photons escaping from the cavity [49, 53–55]. In the open space approach photons not absorbed by the detector were lost in the space while in the cavity field approach every photon (at least in principle) can be detected.

The pioneering work of the cavity field photodetection was made by Srinivas and Davies [53] who considered continuous photodetection and showed that the detection of a single photon is governed by the operator

$$\hat{J}\hat{\rho}(t) = \gamma \hat{a}\hat{\rho}(t)\hat{a}^{\dagger}, \tag{5.1}$$

while the detection of no photons is governed by the operator

$$\hat{S}(\Delta t)\hat{\rho}(t) = e^{(-\mathrm{i}\omega\hat{a}^{\dagger}\hat{a} - \frac{\gamma}{2}\hat{a}^{\dagger}\hat{a})\Delta t}\hat{\rho}(t)e^{(+\mathrm{i}\omega\hat{a}^{\dagger}\hat{a} - \frac{\gamma}{2}\hat{a}^{\dagger}\hat{a})\Delta t}, \tag{5.2}$$

where ω is the field frequency and γ describes the coupling of the field to the detector. The density operator of the field after a short measurement interval $[t, t + \Delta t)$ is given by

$$\hat{\rho}(t + \Delta t) = \hat{J}\hat{\rho}(t)\Delta t + \hat{S}(\Delta t)\hat{\rho}(t). \tag{5.3}$$

Depending on the measurement outcome the state of the field collapses into $\hat{\rho}(t+\Delta t)$ $= \hat{J}\hat{\rho}(t)\Delta t/\text{Tr}\{\hat{J}\hat{\rho}(t)\Delta t\}$ if a photon is detected, or into $\hat{\rho}(t + \Delta t) = \hat{S}(\Delta t)\hat{\rho}(t)/$ $\text{Tr}\{\hat{S}(\Delta t)\hat{\rho}(t)\}$ if nothing is detected. It follows from equation (5.1) that the photon detection rate is $\text{Tr}\{\hat{J}\hat{\rho}(t)\} = \gamma\bar{n}(t)$, where $\bar{n}(t)$ is the expectation value of the number of photons. Therefore, the probability to detect a photon during $[t, t + \Delta t)$ is

$$p_{\text{detect}} = \gamma\bar{n}(t)\Delta t. \tag{5.4}$$

Since equation (5.4) in itself is not bounded to be at most unity, a discussion on the validity of the model has risen especially for the fields with high photon number [56, 57]. However, it immediately follows from equation (5.3) that Δt must be so short that $p_{\text{detect}} + p_{\text{no-detect}} = 1$, since only these two trajectories are accounted in equation (5.3) as we have discussed in publication I. It was also pointed out in [52] that if it is assumed that at most one photon is detected during Δt, Δt is limited by condition

$$\Delta t \ll \frac{1}{\text{detection rate}}. \tag{5.5}$$

In practice, it is not convenient to constrict the detection to infinitesimally short intervals. Therefore, we have defined two practical detector models (see publications I, II and V). The resolving single photon detector (RD) model describes the detection of exactly one photon during a non-differential time interval whereas the non-resolving detector (NRD) model describes the detection of one or more photons during a non-differential time interval. As examples of photon number resolving and non-resolving detectors the photomultiplier tube and avalanche photodiode were given in section 4.2.

Using operators $\hat{J}$ and $\hat{S}$ the operator corresponding to detection of m photons

during $[0, t)$ can be defined as

$$
\begin{aligned}
\hat{C}(t, m)\hat{\rho}(0) &= \int_{t_m=0}^{t} \ldots \int_{t_1=0}^{t_2} \hat{S}(t - t_m)\hat{J}\hat{S}(t_m - t_{m-1})\ldots\hat{J}\hat{S}(t_1)\hat{\rho}(0)\mathrm{d}t_1\ldots\mathrm{d}t_m \\
&= \sum_{n=m}^{\infty} \frac{n!}{m!(n-m)!}\left(1 - e^{-\gamma t}\right)^m \left(e^{-\gamma t}\right)^{n-m} p_n(0)|n-m\rangle\langle n-m|,
\end{aligned}
$$
(5.6)

where $p_n(0)$ is the probability of the n photon Fock state in the mixture $\hat{\rho}(0)$, and $\mathrm{Tr}\{\hat{C}(t, m)\}$ is the probability of counting m photons during $[0, t)$. Only diagonal elements have been written for simplicity since only the diagonal elements are relevant in our calculations. With this result we define the detection operators of the resolving detector ($\hat{C}(t, m = 1)$) and the non-resolving detector ($\sum_{m=1}^{\infty} \hat{C}(t, m)$) as

$$
\hat{C}_{\mathrm{RD}}(t)\hat{\rho}(0) = \sum_{n=0}^{\infty}(n+1)\left(1 - e^{-\gamma t}\right)\left(e^{-\gamma t}\right)^n p_{n+1}(0)|n\rangle\langle n|
$$
(5.7)

$$
\hat{C}_{\mathrm{NRD}}(t)\hat{\rho}(0) = \sum_{m=1}^{\infty}\sum_{n=0}^{\infty}\frac{(n+m)!}{m!n!}\left(1 - e^{-\gamma t}\right)^m \left(e^{-\gamma t}\right)^n p_{n+m}(0)|n\rangle\langle n|.
$$
(5.8)

5.2   Coincidence photon detection

In a coincidence photon detection experiment photons are detected with one detector at consecutive measurement intervals or at the same time with several spatially distributed detectors, or both. The coincidence probabilities are related to the correlation of the photons at the field as will be shown. Using coincidence detections bunching or antibunching phenomena can be revealed. Coincidence detection schemes are considered in publication I.

We define the coincidence detection as a sequence of measurements where one photon is counted at each of the specific non-overlapping intervals $[t_1, t_1 + \mathrm{d}t_1), \ldots, [t_k, t_k + \mathrm{d}t_k)$. Between these intervals the system is assumed to evolve according to the average evolution operator i.e. any number of photons can be absorbed but the detector is not recording. This assumption is made for generality, since e.g. some detectors

have dead times after detection during which they cannot record the absorbed photons. The average evolution operator during $[0, t)$ is obtained using equation (5.6) as [53]

$$\hat{T}_t = \sum_{m=0}^{\infty} \hat{C}(t, m). \tag{5.9}$$

Equation (5.9) accounts for all the possible trajectories of absorbing from zero to infinite photons. Therefore, it corresponds to the evolution given by the master equation (3.1). The probability that the system undergoes the average evolution during $[0, t_1)$ and the one-count occurs during $[t_1, t_1 + \mathrm{d}t_1)$ is $\mathrm{Tr}\{\hat{J}\hat{T}_{t_1}\hat{\rho}(0)\}\mathrm{d}t_1$. After the one-count event the system is projected into the state $\hat{\rho}(t_1 + \mathrm{d}t_1) = \hat{J}\hat{T}_{t_1}\hat{\rho}(0)$ / $\mathrm{Tr}\{\hat{J}\hat{T}_{t_1}\hat{\rho}(0)\}$. The probability of the second one-count event is $\mathrm{Tr}\{\hat{J}\hat{T}_{t_2-t_1}\hat{\rho}(t_1 + \mathrm{d}t_1)\}\mathrm{d}t_2 = \mathrm{Tr}\{\hat{J}\hat{T}_{t_2-t_1}\hat{J}\hat{T}t_1\hat{\rho}(0)\}\mathrm{d}t_2$ / $\mathrm{Tr}\{\hat{J}\hat{T}_{t_1}\hat{\rho}(0)\}$, which is a conditional probability that the trajectory corresponding to the operator $\hat{J}\hat{T}_{t_1}$ has occurred previously. The state now becomes $\hat{\rho}(t_2 + \mathrm{d}t_2) = \hat{J}\hat{T}_{t_2-t_1}\hat{\rho}(t_1 + \mathrm{d}t_1)$ / $\mathrm{Tr}\{\hat{J}\hat{T}_{t_2-t_1}\hat{\rho}(t_1 + \mathrm{d}t_1)\} = \hat{J}\hat{T}_{t_2-t_1}\hat{J}\hat{T}_{t_1}\hat{\rho}(0)$ / $\mathrm{Tr}\{\hat{J}\hat{T}_{t_2-t_1}\hat{J}\hat{T}_{t_1}\hat{\rho}(0)\}$. By using this result recursively we conclude that the probability of the kth event and the density operator after this event are, respectively, given by

$$p(t_k|t_{k-1}, \ldots, t_1) = \frac{\mathrm{Tr}\{\hat{J}\hat{T}_{t_k-t_{k-1}} \ldots \hat{T}_{t_2-t_1}\hat{J}\hat{T}_{t_1}\hat{\rho}(0)\}\mathrm{d}t_k}{\mathrm{Tr}\{\hat{J}\hat{T}_{t_{k-1}-t_{k-2}} \ldots \hat{T}_{t_2-t_1}\hat{J}\hat{T}_{t_1}\hat{\rho}(0)\}} \tag{5.10}$$

$$\hat{\rho}(t_k + \mathrm{d}t_k|t_{k-1}, \ldots, t_1) = \frac{\hat{J}\hat{T}_{t_k-t_{k-1}} \ldots \hat{T}_{t_2-t_1}\hat{J}\hat{T}_{t_1}\hat{\rho}(0)}{\mathrm{Tr}\{\hat{J}\hat{T}_{t_k-t_{k-1}} \ldots \hat{T}_{t_2-t_1}\hat{J}\hat{T}_{t_1}\hat{\rho}(0)\}}. \tag{5.11}$$

Equation (5.10) gives the conditional probability of kth count with the conditions that $k - 1$ one-count events have occurred at $[t_1 + \mathrm{d}t_1), \ldots, [t_{k-1} + \mathrm{d}t_{k-1})$ and any number of photons may have been absorbed between these events.

The probability $p(t_1, \ldots, t_k)$ of the k-count quantum trajectory is the probability of recording k one-count events at times $[t_1, t_1 + \mathrm{d}t_1) \ldots [t_k, t_k + \mathrm{d}t_k)$. It is given by the product of the conditional one-count probabilities so that

$$p(t_1, \ldots, t_k) = \mathrm{Tr}\{\hat{J}\hat{T}_{t_k-t_{k-1}} \ldots \hat{T}_{t_2-t_1}\hat{J}\hat{T}_{t_1}\hat{\rho}(0)\}\mathrm{d}t_1 \ldots \mathrm{d}t_k, \tag{5.12}$$

where the operators $\hat{T}$ allow any number of photon absorptions between these events i.e. the system is under average evolution between the one-count events. We point

out that in defining the probability in equation (5.12) we have used the one-count operator in such a way that $\mathrm{Tr}\{\hat{J}\hat{\rho}(t_i)\mathrm{d}t_i\} \ll 1$, $i = 1, \ldots, k$ i.e. the probability of counting two or more photons at single measurement interval is negligible. For non-differential measurement times this assumption may not hold and operators $\hat{C}_{\mathrm{RD}}$ and $\hat{C}_{\mathrm{NRD}}$ are used instead of $\hat{J}$ as will be done later.

The conditional probability for the kth detection with the condition of $k-1$ previous detections and the probability of coincidence detection of k photons can also be written by using the factorial moments as (details are given in publication I)

$$
\begin{aligned}
p(t_k|t_{k-1}, \ldots, t_1) &= \gamma \frac{\overline{n(n-1)(n-2) \ldots (n-(k-1))}(0)}{\overline{n(n-1)(n-2) \ldots (n-(k-2))}(0)} e^{-\gamma t_k}\mathrm{d}t_k \quad (5.13) \\
p(t_1, t_2, \ldots, t_k) &= \gamma^k \overline{n(n-1) \ldots (n-(k-1))}(0) e^{-\gamma(t_1+\cdots+t_k)}\mathrm{d}t_1 \cdots \mathrm{d}t_k.
\end{aligned}
$$

$$(5.14)$$

Equation (5.14) shows that the k photon coincidence probability is proportional to the kth factorial moment $\overline{n(n-1) \ldots (n-(k-1))}(0)$ of the initial field. The kth factorial moments for the Fock state, coherent field and thermal field are (see section 2.3 for the probability distributions)

$$
\frac{N!}{(N-k)!} \qquad \text{Fock} \qquad (5.15)
$$

$$
\bar{n}^k(0) \qquad \text{Coherent} \qquad (5.16)
$$

$$
k!\bar{n}^k(0) \qquad \text{Thermal,} \qquad (5.17)
$$

where $|N\rangle$ is the initial Fock state and in the case of Fock state $k \leq N$. Assuming that a photon is detected at $[0, \mathrm{d}t)$ the conditional probability of detecting second photon immediately after the first one can be calculated using equation (5.13). The probabilities are

$$
p(\mathrm{d}t|0) = \gamma(N-1)\mathrm{d}t \qquad \text{Fock} \qquad (5.18)
$$

$$
p(\mathrm{d}t|0) = \gamma\bar{n}(0)\mathrm{d}t \qquad \text{Coherent} \qquad (5.19)
$$

$$
p(\mathrm{d}t|0) = 2\gamma\bar{n}(0)\mathrm{d}t \qquad \text{Thermal,} \qquad (5.20)
$$

where dt is assumed so small that $\exp(-\gamma \mathrm{d}t) \approx 1$. Equation (5.4) states that the probability of detecting the first photon is $\gamma \bar{n}(0)\mathrm{d}t$. Comparison of the probabilities shows that the conditional probability of detecting the second photon is (i) smaller than the probability of detecting the first one for Fock state, (ii) equal to the probability of detecting the first one for coherent field, and (iii) is twice the probability of detecting the first one for thermal field. These conditional probabilities express the photon anti-bunching, non-bunching and bunching phenomena for the Fock state, coherent field and thermal field, respectively.

In the derivations of the CP we have assumed that the measurement intervals are so short that the probability of each one-count (detection) event is small, as noted before. However, this might not be a practical assumption for the experiments. Therefore, we will also define the CP using the resolving ($\hat{C}_{\mathrm{RD}}$) and non-resolving ($\hat{C}_{\mathrm{NRD}}$) detector schemes instead of $\hat{J}$. These definitions correspond to detecting exactly one photon and at least one photon during each non-differential intervals $[t_i, t_i + \Delta t_i)$, $i = 1, \ldots, k$. Equations (5.10)–(5.14) can be applied for calculations of the coincidence probabilities of counting exactly one or at least one photons at each of the k intervals by replacing $\hat{J}$ with $\hat{C}_{\mathrm{RD}}$ and $\hat{C}_{\mathrm{NRD}}$, respectively.

In Fig 5.1 we show a comparison of (a) CPs calculated using count operator $\hat{J}$ defined in equation (5.1), (b) CPs obtained using operator $\hat{C}_{\mathrm{RD}}$ defined in equation (5.7) i.e. counting exactly one photon, and (c) CPs obtained using operator $\hat{C}_{\mathrm{NRD}}$ defined in equation (5.8) i.e. counting at least one photon. In this example case the k measurement intervals are chosen so that $[t_i, t_i + \Delta \tau)$, $t_i = (2i-1)\Delta \tau$, $i = 1, \ldots, k$ with $\Delta \tau = 1/(5\gamma)$, and the fields have initially 10 photons. Note that the condition in equation (5.5) is not fulfilled and, therefore, CPs given by equation (5.12) are not well-defined since the measurement intervals are not differential (see Fig. 5.1 (a)). On the contrary, the CPs obtained using the RD and NRD detection schemes are well-defined (see Figs. 5.1 (b) and (c)). These probabilities correspond to detecting exactly one and at least one photon, respectively, at each of the non-differential
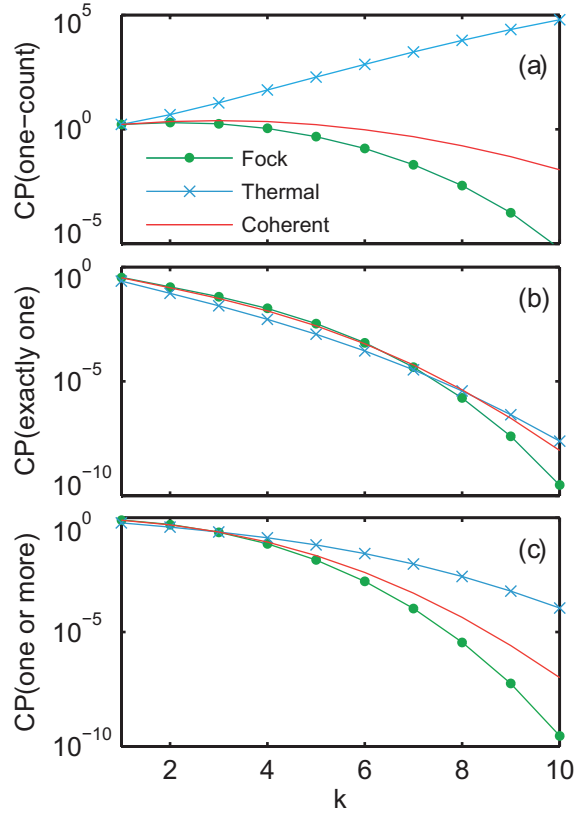
Figure 5.1: (a) The coincidence probabilities of counting k photons one at each measurement interval using operator $\hat{J}$ (equation (5.1)), (b) the coincidence probabilities of counting exactly one photon at each measurement interval using operator $\hat{C}_{\text{RD}}$ (equation (5.7)), and (c) the coincidence probabilities of counting at least one photon at each measurement interval using operator $\hat{C}_{\text{NRD}}$ (equation (5.8)) given for the Fock state, the thermal field and the coherent field. The measurement intervals are chosen so that $[t_i, t_i + \Delta\tau)$, $t_i = (2i - 1)\Delta\tau$, $i = 1, \ldots, k$ with $\Delta\tau = 1/(5\gamma)$. Thus, the field is detected at sequences of $\Delta\tau$ and between these detections the field is assumed to evolve according to the average evolution operator $\hat{T}_{\Delta\tau}$ (corresponding to e.g. the dead time of the detector). The initial expectation value of the number of photons is $\bar{n}(0) = 10$. See publication I for derivations.

measurement intervals.

We also point out that for a differential Δt all the three counting operators ($\hat{J}$, $\hat{C}_{\mathrm{RD}}$ and $\hat{C}_{\mathrm{NRD}}$) give equal results. This is understandable since at a differential measurement interval the only possible trajectories are the detection of zero or one photons. More comparisons of the coincidence probabilities are given in publication I.

5.3 Photon subtraction and addition models and experimental setups

An experimental single photon subtraction scheme was introduced by Parigi *et al.* [4]. The setup is based on a BS and a photodetector (see Fig. 5.2 (a)). A corresponding setup can be used for single photon addition (see Fig. 5.2 (a)). We have studied the single photon subtraction and addition schemes in publications II and V and showed the equivalence of the damped cavity mode model and the BS and photodetector based model. The equivalence is obtained if transmission and reflection probabilities of the BS are set to

$$
\begin{aligned}
T &= \exp(-\gamma t) & (5.21) \\
R &= 1 - \exp(-\gamma t), & (5.22)
\end{aligned}
$$

where γ is the field-detector coupling and t is the interaction time. This relation was obtained also in [28, 58] based on intuitive considerations but with the use of RD and NRD detection schemes we were able to show the exact equivalence. Figure 5.2 (b) shows schematically the correspondence between damped cavity mode and the BS based scheme: each BS for the light pulse corresponds to time Δt in the damped cavity.
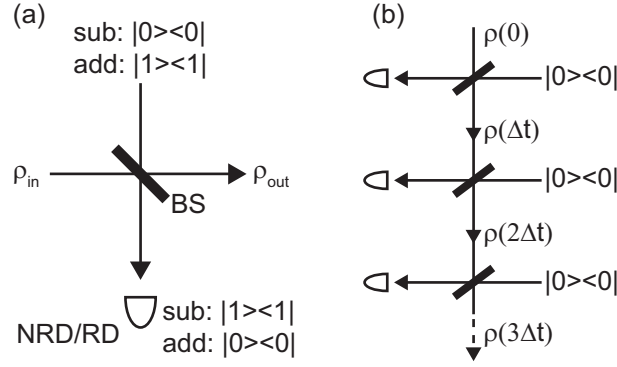
Figure 5.2: (a) Beam splitter based single photon subtraction/addition scheme. *Single photon subtraction*: The input field and a vacuum state are incident on the beam splitter. If exactly one photon is detected from the reflected mode a photon subtraction has taken place (the reflected output is in the state $|1\rangle\langle 1|$). *Single photon addition*: The input field and a single photon Fock state are incident on the beam splitter. If no photons are detected from the reflected mode a photon addition has been accomplished (the reflected output is in the state $|0\rangle\langle 0|$). (b) Beam splitter setup corresponding to the measurement of the cavity field with the fitting $R = 1 - \exp(-\gamma\Delta t)$ and $T = \exp(-\gamma\Delta t)$. Note that Δt is not limited to be differential. See publication II.

5.3.1 Single photon subtraction

The density operator of the photon subtracted state using RD and NRD for detection of the reflected mode, and the density operator after failed subtraction (i.e. zero photons detected from the reflected mode) are

$$\hat{\rho}_{\text{sub,RD}} = \frac{\sum_{n=0}^{\infty} T^n(n+1)p_{n+1}|n\rangle\langle n|}{\sum_{n=0}^{\infty} T^n(n+1)p_{n+1}} \tag{5.23}$$

$$\hat{\rho}_{\text{sub,NRD}} = \frac{\sum_{i=1}^{\infty}\sum_{n=0}^{\infty} \frac{(n+i)!}{i!n!}R^i T^n p_{n+i}|n\rangle\langle n|}{\sum_{i=1}^{\infty}\sum_{n=0}^{\infty} \frac{(n+i)!}{i!n!}R^i T^n p_{n+i}} \tag{5.24}$$

$$\hat{\rho}_{\text{sub,fail}} = \frac{\sum_{n=0}^{\infty} T^n p_n|n\rangle\langle n|}{\sum_{n=0}^{\infty} T^n p_n}, \tag{5.25}$$

where for simplicity only diagonal elements are written since only they are relevant in our calculations. Details of derivation are given in publications II and V. For the thermal field, coherent field, and Fock state the single photon subtraction probabilities and the number of photons in the corresponding photon subtracted states

using RD are (see publication II for details)

$$p_{\text{sub, RD}}^{\text{ther}} = \frac{R\bar{n}_0}{(1 + R\bar{n}_0)^2} \qquad\qquad \bar{n}_{\text{sub, RD}}^{\text{ther}} = \frac{2T\bar{n}_0}{1 + R\bar{n}_0} \qquad (5.26)$$

$$p_{\text{sub, RD}}^{\text{coh}} = R\bar{n}_0 e^{-R\bar{n}_0} \qquad\qquad \bar{n}_{\text{sub, RD}}^{\text{coh}} = T\bar{n}_0 \qquad (5.27)$$

$$p_{\text{sub, RD}}^{\text{Fock}} = RT^{N-1}N \qquad\qquad \bar{n}_{\text{sub, RD}}^{\text{Fock}} = N - 1, \qquad (5.28)$$

where $\bar{n}_0$ is the initial expectation value of the number of photons in the initial thermal and coherent fields, and N is the number of photons in the initial Fock state. In contrast, the single photon subtraction probabilities and the number of photons in the corresponding photon subtracted states using NRD are given by (see publication II for details)

$$p_{\text{sub, NRD}}^{\text{ther}} = \frac{R\bar{n}_0}{1 + R\bar{n}_0} \qquad\qquad \bar{n}_{\text{sub, NRD}}^{\text{ther}} = \frac{T\bar{n}_0(2 + R\bar{n}_0)}{1 + R\bar{n}_0} \qquad (5.29)$$

$$p_{\text{sub, NRD}}^{\text{coh}} = 1 - e^{-R\bar{n}_0} \qquad\qquad \bar{n}_{\text{sub, NRD}}^{\text{coh}} = T\bar{n}_0 \qquad (5.30)$$

$$p_{\text{sub, NRD}}^{\text{Fock}} = 1 - T^N \qquad\qquad \bar{n}_{\text{sub, NRD}}^{\text{Fock}} = \frac{T - T^N}{1 - T^N}N. \qquad (5.31)$$

Figure 5.3 shows comparison of photon detection probabilities and the expectation value of the number of photons in the photon subtracted state. The reflection coefficient of the BS is chosen to $R = 0.01$ as in the experiments of Parigi *et al.* [4]. Note the interesting features that in the regime $R\bar{n}_0 \ll 1$ the number of photons is doubled for field initially in the thermal state (compare to equations (5.26) and (5.29)) as observed experimentally in [4] and, furthermore, for fields in the coherent state the photon number remains invariant (compare equation (5.27) and (5.30)) as is verified experimentally [37]. These surprising phenomena follow from distributions of photons in the thermal and coherent fields (see section 2.3). As noted before, coherent field is an eigenstate of the annihilation operator so it does not change in the photon subtraction. On the other hand, the vacuum state is always the most probable state in the thermal field, so subtraction of single photon projects the field into a state where the initial vacuum state is not present (see also [55]). Thus, the probabilities of the states $|n > 0\rangle$ are increased. Figure 5.4 shows detection probabilities and photon number in the photon subtracted state using NRD with different values of R.
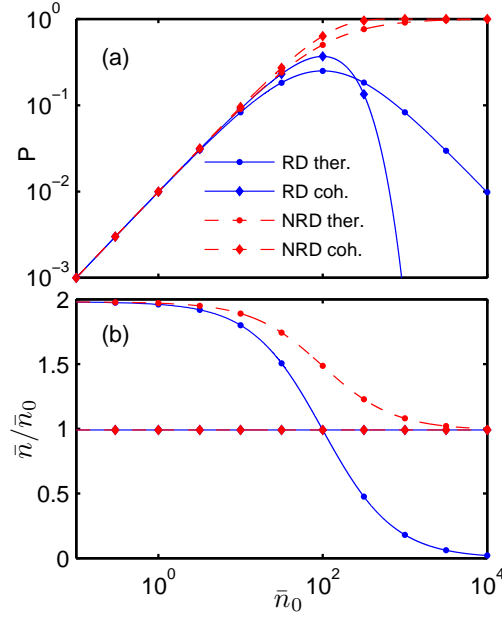
Figure 5.3: Comparison of the RD and NRD detector models. (a) The detection probability and (b) the expectation value of the number of photons after detection as a function of the expectation value of the number of photons ($\bar{n}_0$) in the initial field. For coherent field both detector models give the same expectation values of the number of photons. $R = 0.01$ as in the measurements in Ref. [4]. Note that for $\bar{n}_0 \gg 1$ the probability of detecting only one photon (using RD) goes to zero since it becomes practically impossible to detect only a single photon. See publication II for more details.

5.3.2   Single photon addition

The density operator of the photon added state using the scheme in figure 5.2 (a) and the density operator after failed addition (i.e one or more photons at the reflected mode is detected using NRD) are

$$\hat{\rho}_{\text{add}} = \frac{\sum_{n=0}^{\infty} T^n (n+1) p_n |n+1\rangle\langle n+1|}{\sum_{n=0}^{\infty} T^n (n+1) p_n} \tag{5.32}$$

$$\hat{\rho}_{\text{add,fail}} = \frac{\sum_{i=1}^{\infty} \langle i_2|\hat{B}|1_2\rangle \hat{\rho}_{\text{in}} \langle 1_2|\hat{B}^\dagger|i_2\rangle}{\text{Tr}\{\sum_{i=1}^{\infty} \langle i_2|\hat{B}|1_2\rangle \hat{\rho}_{\text{in}} \langle 1_2|\hat{B}^\dagger|i_2\rangle\}}. \tag{5.33}$$

See publication V for details. In successful addition zero photons are detected from the reflected mode so RD and NRD detector schemes give equal results. For the initial thermal field, coherent field, and Fock state the probabilities of successful single photon addition and the number of photons in the photon added states are (see publication V for details)

$$p_{\text{add}}^{\text{ther}} = \frac{R(\bar{n}_0 + 1)}{(1 + R\bar{n}_0)^2} \qquad\qquad \bar{n}_{\text{add}}^{\text{ther}} = \frac{1 + (1 + T)\bar{n}_0}{1 + R\bar{n}_0} \qquad\qquad (5.34)$$

$$p_{\text{add}}^{\text{coh}} = R(1 + T\bar{n}_0)e^{-R\bar{n}_0} \qquad\qquad \bar{n}_{\text{add}}^{\text{coh}} = \frac{1 + T\bar{n}_0(3 + T\bar{n}_0)}{1 + T\bar{n}_0} \qquad\qquad (5.35)$$

$$p_{\text{add}}^{\text{Fock}} = RT^N(N + 1) \qquad\qquad \bar{n}_{\text{add}}^{\text{Fock}} = N + 1, \qquad\qquad (5.36)$$
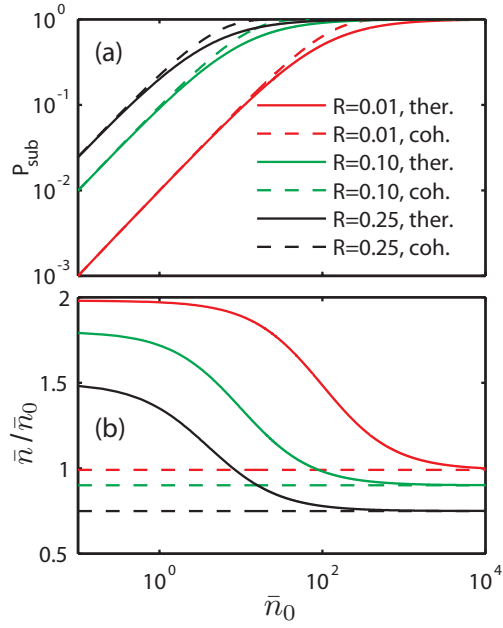
where N is the number of photons in the initial Fock state. The probability of successful single photon addition and the number of photons at the single photon added state for the thermal and coherent fields are shown in figure 5.5. We notice that the number of photons in the photon added state can be larger than $\bar{n}_0 + 1$. In figure 5.4 we have considered single photon subtraction using NRD with different values of R whereas in figure 5.5 single photon addition is considered.

The complement of photon subtraction event using NRD is the detection of zero photons in the reflected mode. In contrast, the complement of the successful single photon addition is the detection of one or more photons using NRD in the reflected mode (cf. figure 5.2). Therefore, the expected measurement output photon number in both cases can be calculated using definition $\bar{n}_{\text{out}} = p_{\text{success}} \cdot \bar{n}_{\text{success}} + p_{\text{fail}} \cdot \bar{n}_{\text{fail}}$ and are given by (see publication V for details)

$$\bar{n}_{\text{sub,out}} = T\bar{n}_0 \qquad\qquad (5.37)$$

$$\bar{n}_{\text{add,out}} = T\bar{n}_0 + R. \qquad\qquad (5.38)$$

Equation (5.37) states that each photon in the input mode is transmitted with probability T to the output mode while equation (5.38) shows that on average the output photon number consists of the input field transmitted with probability T and the added photon reflected with probability R. Thus, in both cases the expected

Figure 5.4: (a) Probability of successful photon subtraction using NRD and (b) the expected number of photons in the photon subtracted state calculated for the thermal and coherent fields with different values of R. Note that when $R\bar{n}_0$ increases the NRD will in practice receive more than a single photon. See publication V for details.
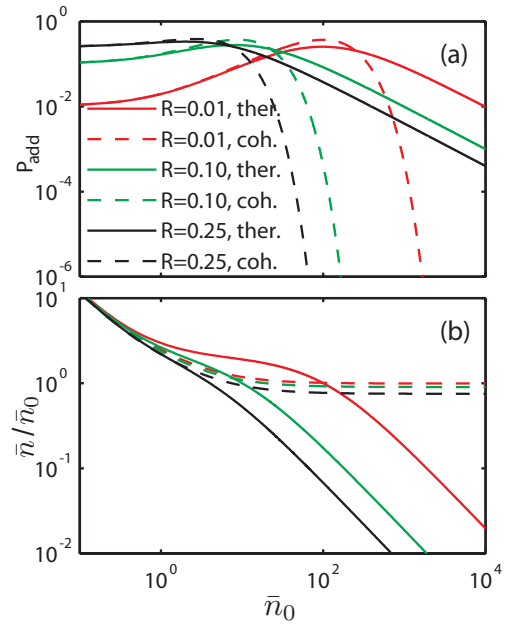
Figure 5.5: (a) Probability of successful single photon addition and (b) the number of photons at the photon added state calculated for the thermal and coherent fields with different values of R. See publication V for details.

output field has fewer photons than the input field even though a single measurement can produce more photons.

6 Dynamics of cavity fields with dissipation and amplification

We will next consider a setup where single mode cavity field is coupled to a reservoir through two state systems. The reservoir can act both as an energy source and as an energy drain. In publications III and IV we have studied purely dissipative case with single two state system, while a purely amplifying setup with single two state system was studied in publication IV. Simultaneous amplification and dissipation was studied in publications V and VI and in the latter one we also generalized the model to setups with multiple two state systems.

6.1 Cavity coupled to a reservoir through two state systems

As before, let γ describe the coupling of the field to a two state system, λ_D describe the relaxation rate of the excited state $|e\rangle$ of the two state system into the reservoir, and λ_A describe the excitation rate of the ground state $|g\rangle$ of the two state system by the reservoir. The density operator $\hat{\rho}_{\text{tot}}$ describing both the field and N_s two state systems evolves according to the Lindblad master equation

$$\frac{\mathrm{d}\hat{\rho}_{\text{tot}}(t)}{\mathrm{d}t} = -\frac{\mathrm{i}}{\hbar}\left(\hat{H}\hat{\rho}_{\text{tot}}(t) - \hat{\rho}_{\text{tot}}(t)\hat{H}^{\dagger}\right) + \sum_{i=1}^{N_s}\left(2\lambda_D\sigma_-^{(i)}\hat{\rho}_{\text{tot}}(t)\sigma_+^{(i)} + 2\lambda_A\sigma_+^{(i)}\hat{\rho}_{\text{tot}}(t)\sigma_-^{(i)}\right).$$

(6.1)

Operators $2\lambda_D\sigma_-^{(i)}\hat{\rho}_{\text{tot}}(t)\sigma_+^{(i)}$ and $2\lambda_A\sigma_+^{(i)}\hat{\rho}_{\text{tot}}(t)\sigma_-^{(i)}$ describe the relaxation and excitation of ith two state system. The Hamiltonian is the Jaynes-Cummings Hamiltonian of two state systems with eigenenergies $\pm\hbar\omega_0/2$ coupled to a photon mode having frequency ω with additional terms describing the reservoir couplings

$$\hat{H} = \frac{1}{2}\hbar\omega_0\sigma_0 + \hbar\omega\hat{a}^{\dagger}\hat{a} + \hbar\gamma\sum_{i=1}^{N_s}\left(\hat{a}\sigma_+^{(i)} + \hat{a}^{\dagger}\sigma_-^{(i)}\right) - \mathrm{i}\hbar\sum_{i=1}^{N_s}\left(\lambda_D\sigma_+^{(i)}\sigma_-^{(i)} + \lambda_A\sigma_-^{(i)}\sigma_+^{(i)}\right).$$

(6.2)

Term $i\hbar\lambda_D\sigma_+\sigma_-$ describes the dissipative coupling where the dissipation event is the relaxation of the two state system. The term $i\hbar\lambda_A\sigma_-\sigma_+$ accounts for the amplification so that the energy adding event is the excitation of the two state system by the reservoir. Furthermore, exact resonance is assumed ($\omega = \omega_0$) and $\sigma_\pm^{(i)}$ operates on the ith two state system. We have also assumed that each two state system has equal coupling constants λ_A, λ_D, and γ.

6.2   Dissipation and amplification rates of the reduced system

Our purpose was to derive a reduced model for the optical field i.e. to obtain a model for the field alone by averaging the two state system out of the density operator but still capture its effect on the field. The reduced dissipation and amplification rates for a system with single two state system, $N_s = 1$, are (details of the derivation are given in publications III, IV and VI)

$$r_D = 2\lambda_D \sum_{n=0}^{\infty} \frac{\frac{\lambda_A}{\lambda_D+\lambda_A} + \left(\frac{\gamma}{\lambda_D+\lambda_A}\right)^2 n}{1 + 2\left(\frac{\gamma}{\lambda_D+\lambda_A}\right)^2 n} p_n \tag{6.3}$$

$$r_A = 2\lambda_A \sum_{n=0}^{\infty} \frac{\frac{\lambda_D}{\lambda_D+\lambda_A} + \left(\frac{\gamma}{\lambda_D+\lambda_A}\right)^2 (n+1)}{1 + 2\left(\frac{\gamma}{\lambda_D+\lambda_A}\right)^2 (n+1)} p_n. \tag{6.4}$$

Setting $\lambda_A = 0$ the purely dissipative system is recovered whereas setting $\lambda_D = 0$ results in the purely amplifying setup. These rates correspond to using quantum jump superoperators of the form

$$\hat{J}_D\hat{\rho} = A_D\hat{O}\hat{\rho}\hat{O}^\dagger \tag{6.5}$$

$$\hat{J}_A\hat{\rho} = A_A\hat{O}^\dagger\hat{\rho}\hat{O}, \tag{6.6}$$

where

$$\hat{O} = \frac{1}{\sqrt{1+B\hat{a}\hat{a}^\dagger}}\hat{a} \tag{6.7}$$

$$B = 2\frac{\gamma^2}{(\lambda_D+\lambda_A)^2}, \quad A_A = \lambda_A B \quad \text{and} \quad A_D = \lambda_D B. \tag{6.8}$$

The form of the operator $\hat{O}$ is a result of the reduced two state system that couples the field and the reservoir. It obeys the following relations

$$\hat{O}|n\rangle = \sqrt{\frac{n}{1+Bn}}|n-1\rangle \qquad \hat{O}^\dagger|n\rangle = \sqrt{\frac{n+1}{1+B(n+1)}}|n+1\rangle \qquad (6.9)$$

$$\hat{O}^\dagger\hat{O}|n\rangle = \frac{n}{1+Bn}|n\rangle \qquad \hat{O}\hat{O}^\dagger|n\rangle = \frac{n+1}{1+B(n+1)}|n\rangle. \qquad (6.10)$$

The reduced master equation for the field can now be written as

$$\frac{\mathrm{d}\hat{\rho}}{\mathrm{d}t} = -\frac{A_D}{2}\left(\hat{O}^\dagger\hat{O}\hat{\rho} - 2\hat{O}\hat{\rho}\hat{O}^\dagger + \hat{\rho}\hat{O}^\dagger\hat{O}\right) - \frac{A_A}{2}\left(\hat{O}\hat{O}^\dagger\hat{\rho} - 2\hat{O}^\dagger\hat{\rho}\hat{O} + \hat{\rho}\hat{O}\hat{O}^\dagger\right). \quad (6.11)$$

The predictions of the reduced model will be compared to the numerical solution of the full system later in figure 6.5.

6.3   Ideal detector setup

By setting $\lambda_A = 0$ we obtain an ideal detector setup which assumes that each jump can be recorded and the cavity is assumed ideal. Later, we will also include cavity losses. In section 5.1 we discussed the model by Srinivas and Davies [53] (SD) where the photon counting operator and the count rate are

$$\hat{J}_{sd}\hat{\rho}(t) = \gamma_{sd}\hat{a}\hat{\rho}(t)\hat{a}^\dagger, \qquad\qquad r_{sd}(t) = \gamma_{sd}\bar{n}(t). \qquad (6.12)$$

In the SD model the count rate is proportional to the number of photons and it is assumed that the detector can absorb photons at unlimited rate. This kind of setup could be achieved e.g. by detecting photons escaping the cavity with PMTs or using a multiplexed detector system where the incoming photon beam is divided into several APDs using BSs [41, 59]. In contrast to the SD model, a model, called the E model, for saturated detectors was discussed in [56, 57, 60–63] with

$$\hat{J}_e\hat{\rho}(t) = \gamma_e\hat{E}\hat{\rho}(t)\hat{E}^\dagger, \qquad\qquad r_e(t) = \gamma_e(1 - p_0(t)), \qquad (6.13)$$

where $\hat{E} = (\hat{a}^\dagger\hat{a} + 1)^{-1/2}\hat{a}$. In the E model the count rate is proportional to the probability that there are photons in the cavity which implies perfect saturation

of the detector. We showed (in publication III and in [64]) that master equation (6.1) reproduces the results predicted by (i) the SD model with $\gamma_{\text{sd}} = 2\gamma^2/\lambda_D$ in the regime $\lambda_D/\gamma \gg \sqrt{\bar{n}}$, and (ii) the E model with $\gamma_{\text{e}} = \lambda_D$ in the regime $\lambda_D/\gamma \ll \sqrt{\bar{n}}$. A comparison of the SD and E field models with numerical solution of equation (6.1) are shown in figure 6.1. The numerical solutions are calculated using the method described in sections 2.5.1–2.5.2.
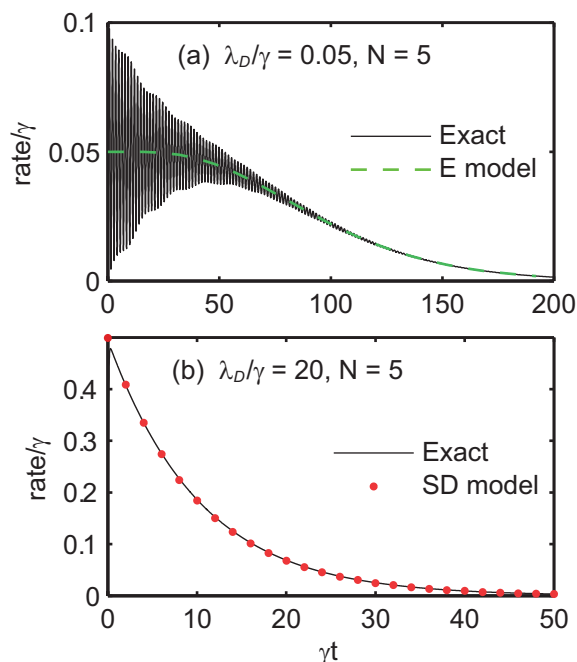

Figure 6.1: The detection rate with two different ratios of the coupling constants: (a) $\lambda_D/\gamma = 0.05$ and (b) $\lambda_D/\gamma = 20$. The field being initially in the Fock state $|5\rangle$. The numerically calculated exact rate from the Lindblad equation (equation (6.1)) (solid line) is compared to the rate given by the E model (equation (6.13), dashed line) and to the rate given by the SD model (equation (6.12), dots). See publication III for details.

Our general reduced photon counting model governed by QJS in equation (6.5) with
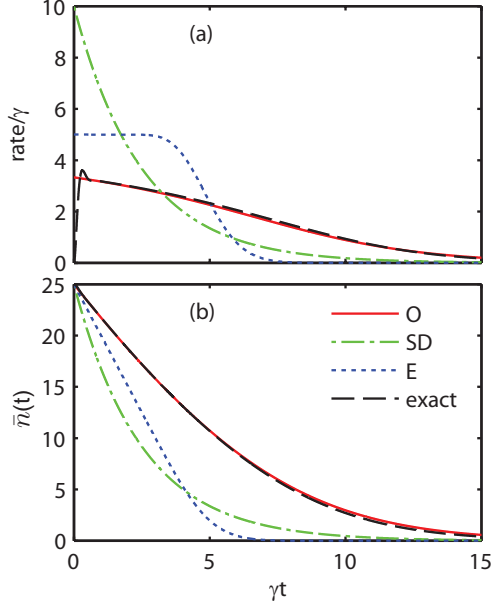
Figure 6.2: (a) The photon counting rates, and (b) the expectation values of the number of photons for a setup with $\lambda_D/\gamma = 5$ and the field initially in the Fock state $|25\rangle$. The coupling strength in the figures are between the strong and weak coupling regimes where neither the SD nor the E model are accurate. As a result they are unable to correctly predict the average dissipation rate and the photon number in the cavity. In contrast our model accurately reproduces these average quantities. See publication IV for details.
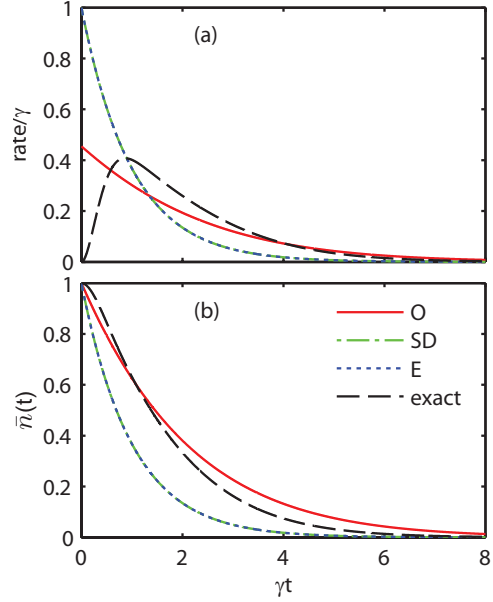
Figure 6.3: (a) The photon counting rates, and (b) the expectation values of the number of photons for a setup with $\lambda_D/\gamma = 2$ and the field initially in the thermal field with $\bar{n}(0) = 1$. Note that in this special case the SD and the E model coincide. Again, the coupling strength in the figures has been chosen to the region where neither the SD nor the E model applies. However, our model is able to predict qualitatively the field evolution, although its accuracy is slightly reduced due to the relatively strong peak in the rate caused by the Rabi type oscillation combined with the fast decay rate. See publication IV for details.

$\lambda_A = 0$ gives

$$\hat{J}\hat{\rho}(t) = A_D \hat{O}\hat{\rho}(t)\hat{O}^\dagger, \qquad r(t) = \sum_{n=1}^{\infty} \frac{\frac{2\gamma^2}{\lambda_D}n}{1 + 2\left(\frac{\gamma}{\lambda_D}\right)^2 n} p_n. \qquad (6.14)$$

In the limit $\gamma/\lambda_D \ll 1$ our model coincides with SD model while in the limit $\gamma/\lambda_D \gg$ 1 the E model is reproduced. Furthermore, in the intermediate regime where neither the SD nor the E model is accurate our reduced model can reproduce the results of the full cavity field-two state system-reservoir setup. Figures 6.2 and 6.3 show comparison of the three reduced models with the full setup at the intermediate regime. Note however that, even though our model can reproduce the average evolution of the full setup, it cannot reproduce the Rabi oscillations. See publication IV for more details and derivations.

Relation between the reduced count rate in equation (6.14) and dissipation rate of the two state system obtained from equation (6.1), $r(t) = 2\lambda p_e(t)$, allows us to define the average excited state probability and the average ground state probability as

$$\bar{p}_e = \sum_{n=0}^{\infty} \frac{\left(\frac{\gamma}{\lambda_D}\right)^2 n}{1 + 2\left(\frac{\gamma}{\lambda_D}\right)^2 n} p_n \qquad (6.15)$$

$$\bar{p}_g = \sum_{n=0}^{\infty} \frac{1 + \left(\frac{\gamma}{\lambda_D}\right)^2 n}{1 + 2\left(\frac{\gamma}{\lambda_D}\right)^2 n} p_n. \qquad (6.16)$$

We show a comparison of the average probabilities of the two state system with the exact probabilities in figure 6.4. In this example case $\lambda_D/\gamma = 0.5$ and the field is initially in the Fock state $|2\rangle$. Again our model reproduces the average evolution but cannot reproduce the Rabi oscillations.

6.4   Multiple two state system

The results obtained for setups with a single two state system can be generalized straightforwardly to setups with multiple two state systems ($N_s > 1$ in equations
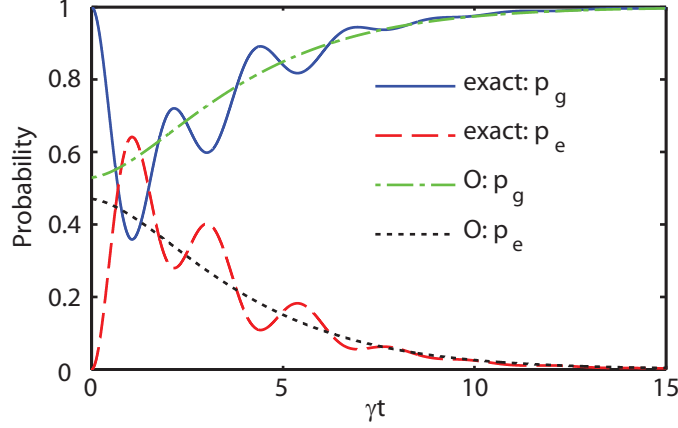
Figure 6.4: Comparison of the excited state probabilities and the ground state probabilities calculated with the full model (exact) and using equations (6.15) and (6.16) for a system with $\lambda_D/\gamma = 0.5$ and field initially in the Fock state $|2\rangle$. See publication IV for details.

(6.1) and (6.2)), since we assume that the two state systems do not interact with each other directly, they only interact with the field and with the reservoir. Furthermore, we assume that each two state system has the same coupling constants λ_A, λ_D, and γ. With these assumptions the reduced master equation (6.11) can be generalized for multiple two state systems by adding separate dissipative and amplifying terms for each of the two state systems. Since the terms are equal due to the equal coupling constants, the reduced master equation generalized for multiple two state systems is obtained by scaling the A parameters with N_S as

$$A_D = \frac{2\lambda_D\gamma^2 N_s}{(\lambda_D + \lambda_A)^2} \tag{6.17}$$

$$A_A = \frac{2\lambda_A\gamma^2 N_s}{(\lambda_D + \lambda_A)^2} \tag{6.18}$$

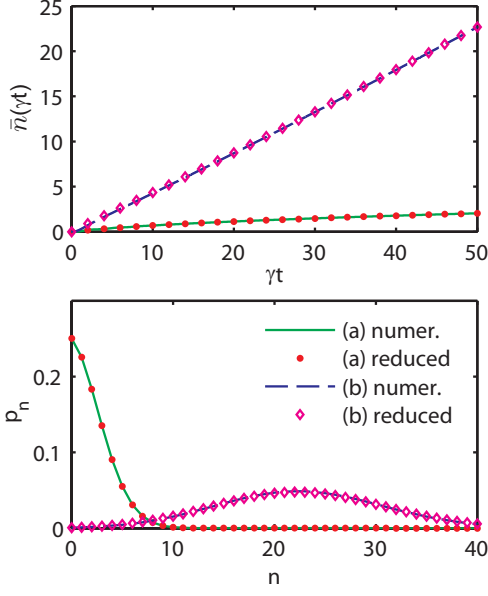$$B = \frac{2\gamma^2}{(\lambda_D + \lambda_A)^2}. \tag{6.19}$$

Figure 6.5 shows the comparison of reduced and full models for setup with $N_s = 1$. In case (a) $\lambda_D = 0.1\gamma$ and $\lambda_A = 0.1\gamma$ and in case (b) $\lambda_D = 0.5\gamma$ and $\lambda_A = 1.0\gamma$. In figure 6.6 we show the comparison of reduced and full models for setup with

$N_s = 3$. The expectation value of the number of photons and the photon distribution are calculated with three different parameter sets: (a) $\lambda_D = 1.0\gamma$, $\lambda_A = 1.0\gamma$ and $\hat{\rho}(0) = |0\rangle\langle 0|$, (b) $\lambda_D = 2.0\gamma$, $\lambda_A = 3.0\gamma$ and $\hat{\rho}(0) = |0\rangle\langle 0|$, (c) $\lambda_D = 0.5\gamma$, $\lambda_A = 0$ and $\hat{\rho}(0) = |10\rangle\langle 10|$. The two state systems are initially in the ground state. The reduced model reproduces the results of the full model except for the Rabi type oscillations (case (c) in Fig. 6.6) as we also pointed out in the previous section. However, for $N_s \gg 1$ the phases of the two state systems in real systems are randomly distributed and the Rabi oscillation are expected to be averaged out naturally and the reduced model is expected to be even more accurate.

6.5 Non-ideal cavity

So far we have assumed an ideal cavity in the sense that all dissipation has been caused by the coupling of the two state systems to the reservoir. To make the model more general, we also include mirror losses of the cavity (see publications IV, V and VI). The mirror losses are taken into account by adding a linear (with respect to the photon number) jump term $C\hat{a}\hat{\rho}\hat{a}^\dagger$ to the reduced master equation. Parameter $C = \omega/Q$, where ω is the frequency of the cavity mode and Q is the quality factor of the cavity [7]. The loss parameter can also be defined as $C = -c/L\ln(R)$ [65], where L is the length of the cavity and R is the reflection probability of the cavity mirrors. The reduced master equation for the field including mirror losses is given by

$$
\begin{aligned}
\frac{\mathrm{d}\hat{\rho}}{\mathrm{d}t} &= -\frac{A_D}{2}\left(\hat{O}^\dagger\hat{O}\hat{\rho} - 2\hat{O}\hat{\rho}\hat{O}^\dagger + \hat{\rho}\hat{O}^\dagger\hat{O}\right) - \frac{A_A}{2}\left(\hat{O}\hat{O}^\dagger\hat{\rho} - 2\hat{O}^\dagger\hat{\rho}\hat{O} + \hat{\rho}\hat{O}\hat{O}^\dagger\right) \\
&\quad - \frac{C}{2}\left(\hat{a}^\dagger\hat{a}\hat{\rho} - 2\hat{a}\hat{\rho}\hat{a}^\dagger + \hat{\rho}\hat{a}^\dagger\hat{a}\right).
\end{aligned}
\tag{6.20}
$$

Figure 6.5: Comparison of the reduced model and the numerical solution of the full system. In case (a) $\lambda_D = 0.1\gamma$ and $\lambda_A = 0.1\gamma$ and in case (b) $\lambda_D = 0.5\gamma$ and $\lambda_A = 1.0\gamma$. The upper figure shows the expectation values of the number of photons while the lower figure shows the photon distribution at $\gamma t = 50$. The full system was initially in the state $|g, 0\rangle$ and the reduced system in the state $|0\rangle$. Note that the solution given by the reduced model accurately follows the exact solution. See publication VI for details.
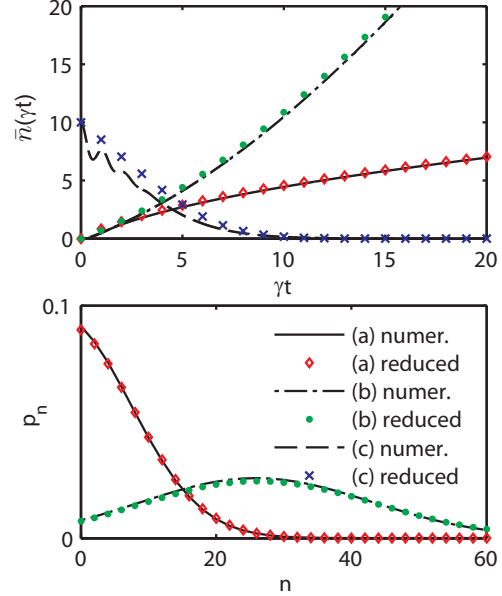
Figure 6.6: Comparison of the reduced model and the full model with 3 two state systems. The upper figure shows the expectation value of the number of photons and the lower figure shows the photon distribution at $\gamma t = 20$. (a) $\lambda_D = 1.0\gamma$, $\lambda_A = 1.0\gamma$ and $\hat{\rho}(0) = |0\rangle\langle 0|$, (b) $\lambda_D = 2.0\gamma$, $\lambda_A = 3.0\gamma$ and $\hat{\rho}(0) = |0\rangle\langle 0|$, and (c) $\lambda_D = 0.5\gamma$, $\lambda_A = 0$ and $\hat{\rho}(0) = |10\rangle\langle 10|$. The two state systems are initially in the ground state. The probability distributions in case (c) are not shown since $p_0 = 1$. See publication VI for details.

From this equation we can obtain the following differential equation for the probability of having n photons in the field

$$
\begin{aligned}
\frac{\mathrm{d}p_n(t)}{\mathrm{d}t} = {} & -\frac{A_D n}{1+Bn}p_n - \frac{A_A(n+1)}{1+B(n+1)}p_n - Cnp_n \\
& + \frac{A_D(n+1)}{1+B(n+1)}p_{n+1} + \frac{A_A n}{1+Bn}p_{n-1} + C(n+1)p_{n+1}.
\end{aligned} \tag{6.21}
$$

We will use equation (6.21) to calculate the steady state solutions of the field in different parameter regimes.

6.6   Steady state solution of the reduced model

The steady state solution of equation (6.21) obtained using the detailed balance condition (rate from state $|n\rangle$ to state $|n+1\rangle$ equals the rate from state $|n+1\rangle$ into state $|n\rangle$) is

$$
p_n = p_0 \prod_{k=1}^{n} \frac{\frac{A_A}{A_D+C}}{1+\frac{BC}{A_D+C}k} \tag{6.22}
$$

with

$$
p_0 = \left(\sum_{n=0}^{\infty} \prod_{k=1}^{n} \frac{\frac{A_A}{A_D+C}}{1+\frac{BC}{A_D+C}k} \right)^{-1}. \tag{6.23}
$$

The steady state photon number and the second order coherence degree are (see publications IV and VI for details)

$$
\bar{n}_{ss} = \frac{A_A - (A_D+C)}{BC} + \frac{A_D+C}{BC}p_0 \tag{6.24}
$$

$$
g_{ss}^{(2)} = \frac{\left[\frac{A_A-(A_D+C)}{BC}\right]\left[\frac{A_A-(A_D+C)}{BC} + \frac{A_D+C}{BC}p_0\right] + \frac{A_D+C}{BC}(1-p_0)}{\left[\frac{A_A-(A_D+C)}{BC} + \frac{A_D+C}{BC}p_0\right]^2}. \tag{6.25}
$$

6.6.1   LED and laser operation

Depending on the relative magnitudes of the energy injection rate A_A into the field, the loss rate A_D due to the active material, and the mirror losses C of the cavity,

our reduced model can reproduce the operation of active optical components.

If amplification is smaller than losses $A_A < A_D + C$ without saturation, $BC \ll A_D + C$, equation (6.22) can be simplified into

$$p_n = \left(1 - \frac{A_A}{A_D + C}\right)\left(\frac{A_A}{A_D + C}\right)^n \tag{6.26}$$

$$\bar{n}_{ss,\text{ther}} = 1/\left(\frac{A_D + C}{A_A} - 1\right), \tag{6.27}$$

which corresponds to a thermal field with $\frac{A_D + C}{A_A} = \exp\left(\frac{\hbar\omega}{k_B T}\right)$, where k_B is the Boltzmann constant and T is the temperature. Thus, under these conditions, the setup operates as an LED. If, on the other hand, amplification is greater than losses $A_A > A_D + C$ and the saturation factor is significant, $BC \gg A_D + C$, we obtain

$$p_n = e^{-\lambda_A/C}\frac{(\lambda_A/C)^n}{n!} \tag{6.28}$$

$$\bar{n}_{ss,\text{coh}} = \lambda_A/C, \tag{6.29}$$

which is the Poisson distribution and, therefore, a coherent field is obtained. In this regime the setup operates as a laser.

6.6.2 Relation of the reservoir temperature to the coupling parameters

The relation of coupling parameters λ_D and λ_A to the temperature of the reservoir can be found by considering a single mode optical field interacting with a thermal reservoir (see publication VI). It is assumed that the cavity mode interacts only with the reservoir and, therefore, all dissipation and energy injection is due to the reservoir. The evolution of the field is governed by the following Lindblad master equation [7]

$$\begin{aligned}
\frac{\mathrm{d}\hat{\rho}}{\mathrm{d}t} &= -\frac{\xi}{2}\bar{n}_{th}\left(\hat{a}\hat{a}^\dagger\hat{\rho} - 2\hat{a}^\dagger\hat{\rho}\hat{a} + \hat{\rho}\hat{a}\hat{a}^\dagger\right) \\
&\quad -\frac{\xi}{2}\left(\bar{n}_{th} + 1\right)\left(\hat{a}^\dagger\hat{a}\hat{\rho} - 2\hat{a}\hat{\rho}\hat{a}^\dagger + \hat{\rho}\hat{a}^\dagger\hat{a}\right),
\end{aligned} \tag{6.30}$$

where ξ is the coupling and $\bar{n}_{th}$ is the mean number of photons in the thermal reservoir. The steady state solution is of course a thermal field with $\bar{n}_{th}$ photons. To compare our model to this result we assume that the cavity mirrors are perfect ($C = 0$) and that the amplification is smaller than dissipation ($A_A < A_D$). We obtain probabilities $p_n = [(\lambda_D - \lambda_A)/\lambda_D](\lambda_A/\lambda_D)^n$ and, furthermore, the steady state photon number is $\bar{n}_{ss} = \left(\frac{\lambda_D}{\lambda_A} - 1\right)^{-1} = \bar{n}_{th} = \left(\exp\left(\frac{\hbar\omega}{k_B T}\right) - 1\right)^{-1}$. Comparison shows that

$$\frac{\lambda_D}{\lambda_A} = \exp\left(\frac{\hbar\omega}{k_B T}\right), \tag{6.31}$$

which means that adjusting the excitation and de-excitation rates of the two state system corresponds to setting the temperature of the reservoir.

6.7 Comparison to semiconductor devices

In semiconductors the absorption and emission rates are given by [50, 51] $r_{\mathrm{abs}} = W(1 - f_e)(1 - f_h)\bar{n}$ and $r_{\mathrm{em}} = W f_e f_h(\bar{n} + 1)$, respectively where W is a material dependent constant, and f_e and f_h are the electron and hole occupation probabilities in the conduction and valence bands, respectively. By comparing these rates to the rates given by our reduced model in equation (6.11) we obtain equations

$$\sum_{n=0}^{\infty} \frac{A_D n}{1 + Bn} p_n = W(1 - f_e)(1 - f_h)\bar{n} \tag{6.32}$$

$$\sum_{n=0}^{\infty} \frac{A_A(n + 1)}{1 + B(n + 1)} p_n = W f_e f_h(\bar{n} + 1). \tag{6.33}$$

Since we have three parameters in our model we need a third equation to solve them. The steady state photon number for semiconductor devices can be solved from equation emission = absorption + mirror losses which gives $\bar{n}_{ss} = W f_e f_h / [W(1 - f_e)(1 - f_h) + C - W f_e f_h]$. Setting $\bar{n}_{ss}$ in this solution equal to $\bar{n}_{ss}$ obtained from equations (6.23) and (6.24) gives the third equation. Using these three relations enables us to solve A_A, A_D and B as a functions of f_e, f_h, and W. A purely amplifying system ($A_D = 0$) is recovered when $f_e = 1$ or $f_h = 1$ and a purely

dissipative system ($A_A = 0$) when $f_h = 0$ or $f_e = 0$. Solving equation (6.32) and (6.33) is generally not straightforward analytically. However, for the two limiting cases of a purely spontaneous emission and a laser field, the parameters can be obtained in simple forms as shown below.

From small fields in the regime $B\bar{n} \ll 1$ it is straightforward to approximate the parameters A_D, A_A and B as (see publication VI)

$$A_D = W(1 - f_e)(1 - f_h) \tag{6.34}$$

$$A_A = W f_e f_h \tag{6.35}$$

$$B \approx 0. \tag{6.36}$$

For laser fields we use equation (6.29) to write $B = A_A/(C\bar{n}_{ss})$ and substitute it to equation (6.32) and (6.33) giving

$$\sum_{n=0}^{\infty} \frac{A_D n}{1 + \frac{A_A n}{C\bar{n}_{ss}}} p_n \approx \frac{A_D}{1 + A_A/C}\bar{n} = W(1 - f_e)(1 - f_h)\bar{n} \tag{6.37}$$

$$\sum_{n=0}^{\infty} \frac{A_A(n+1)}{1 + \frac{A_A(n+1)}{C\bar{n}_{ss}}} p_n \approx \frac{A_A}{1 + A_A/C}(\bar{n} + 1) = W f_e f_h(\bar{n} + 1), \tag{6.38}$$

where we have assumed the distribution to be narrow at $\bar{n}_{ss}$ so that $n/\bar{n}_{ss} \approx 1$ in the denominators. Parameters A_D, A_A and B can now be evaluated as

$$A_D = \frac{W(1 - f_e)(1 - f_h)}{1 - \frac{W f_e f_h}{C}} \tag{6.39}$$

$$A_A = \frac{W f_e f_h}{1 - \frac{W f_e f_h}{C}} \tag{6.40}$$

$$B = \frac{A_A}{C\bar{n}_{ss}}, \tag{6.41}$$

where $\bar{n}_{ss} = W f_e f_h / [W(1 - f_e)(1 - f_h) + C - W f_e f_h]$.

7 Conclusions

The Lindblad master equation is a standard model used to predict the time evolution of open quantum systems. In the publications presented in this summary, we have applied the Lindblad master equation to study the relaxation of an optical cavity field and derived general quantum jump superoperators that on average correctly describe the dynamics of the field and significantly simplify the treatment of the cavity field dynamics. The systems we have studied consist of the optical cavity field coupled to amplifying and/or dissipative reservoirs through one or more atomic two state systems. The studied system is fairly general and we have used it to describe photodetectors, LEDs and lasers.

We have generalized the single photon counting quantum jump superoperator for two experimentally feasible schemes. The resolving detection model corresponds to detection of exactly one photon while the non-resolving detection model corresponds to detection of one or more photons. Both models are applicable to fields from the quantum limit to the classical limit and from the weak to the strong coupling regimes. The RD and NRD detector schemes have been applied to model coincidence detection experiments. We also showed that, by equating the reflection probability of the BS with the absorption probability of a photon and the transmission probability of the BS with the probability that a photon is not absorbed, the cavity field model and the BS based schemes are equivalent in photon subtraction and creation experiments.

We have also derived a reduced model for the cavity fields coupled to a reservoir through two state systems. The two state systems can inject energy from the reservoir into the field and also dissipate the energy of the field into the reservoir. At the purely dissipative regime our model reproduces the previously introduced models of non-saturated and fully saturated detectors depending on relative strengths of the

field-two state system coupling and the two state system-reservoir coupling. Taking also the mirror losses of the cavity into account, we have shown that our dynamic model creates a laser field if the amplification is greater than the losses. Below the threshold a thermal field is produced and the system operates as an LED. Furthermore, we have shown that our model can be used to model semiconductor devices by replacing our model parameters with the parameters of the semiconductor device.

The derived models can be applied to a wide variety of cavity field experiments. In addition to the optical fields of semiconductor devices, our model is applicable to cavity field based quantum information processing experiments. Furthermore, fundamental quantum optics experiments of single photon addition, single photon subtraction, coincidence detection, and their combinations can be analyzed using the derived models.

References

[1] R. Hanbury Brown and R. Q. Twiss. Correlation between photons in two coherent beams of light. *Nature*, 177:27–29, 1956.

[2] R. J. Glauber. *Quantum Theory of Optical Coherence.* Wiley-VHC, 2007.

[3] R. J. Glauber. The quantum theory of optical coherence. *Physical Review*, 130(6):2529 – 2539, 1963.

[4] V. Parigi, A. Zavatta, M. Kim, and M. Bellini. Probing quantum commutation rules by addition and subtraction of single photons to/from a light field. *Science*, 317(5846):1890–1893, 2007.

[5] A. I. Lvovsky, B. C. Sanders, and W. Tittel. Optical quantum memory. *Nature Photonics*, 3(12):706–714, 2009.

[6] R. Loudon. *The Quantum Theory of Light.* Oxford University Press, 1983.

[7] M. O. Scully and M. S. Zubairy. *Quantum Optics.* Cambridge University Press, 1997.

[8] A. B. Klimov and S. M. Chumakov. *A Group-Theoretical Approach to Quantum Optics.* Wiley-VCH, 2009.

[9] R. L. Liboff. *Introductory Quantum Mechanics.* Addison-Wesley, third edition, 1998.

[10] W. P. Schleich. *Quantum Optics in Phase Space.* Wiley-VCH, 2001.

[11] C. W. Gardiner and P. Zoller. *Quantum Noise.* Springer, third edition, 2004.

[12] H.-P. Breuer and F. Petruccione. *The Theory of Open Quantum Systems.* Oxford University Press, 2006.

[13] Y. Yamamoto and A. Imamoglu. *Mesoscopic Qauntum Optics.* John Wiley & Sons, 1999.

[14] E. T. Jaynes and F. W. Cummings. Comparison of quantum and semiclassical radiation theories with application to the beam maser. *Proceedings of the IEEE*, 51(1):89–109, 1963.

[15] S. Stenholm. Quantum theory of electromagnetic fields interacting with atoms and molecules. *Physics Reports*, 6(1):1–122, 1973.

[16] B. Shore and P. Knight. The Jaynes-Cummings model. *Journal of Modern Optics*, 40(7):1195–1238, 1993.

[17] J.-S. Peng and G.-X. Li. *Introduction to Modern Quantum Optics.* World Scientific, 1998.

[18] L. Mandel. Sub-poissonian photon statistics in resonance fluorescence. *Optics Letters*, 4(7):205–207, 1979.

[19] X.-Z. Zhang, Z.-H. Wang, H. Li, Q. Wu, B.-Q. Tang, F. Gao, and J.-J. Xu. Characterization of photon statistical properties with normalized Mandel parameter. *Chinese Physics Letters*, 25(11):3976, 2008.

[20] U. Leonhardt. Quantum physics of simple optical instruments. *Reports on Progress in Physics*, 66:1207–1249, 2003.

[21] G. Lindblad. On the generators of quantum dynamical semigroups. *Communications in Mathematical Physics*, 48:119–130, 1976.

[22] J. S. Marsh. Explicit measurement theory for quantum mechanics. *Physical Review A*, 64(4):042109, 2001.

[23] H. J. Carmichael. *An open system approach to Quantum Optics.* Springer-Verlag, 1993.

[24] S. Stenholm and K.-A. Suominen. *Quantum approach to informatics.* John Wiley & Sons, 2005.

[25] M. S. Kim, W. Son, V. Bužek, and P. L. Knight. Entanglement by a beam splitter: Nonclassicality as a prerequisite for entanglement. *Physical Review A*, 65(3):032323, 2002.

[26] V. Parigi, A. Zavatta, M. Kim, and M. Bellini. Supporting Online Material of Ref. [4].

[27] U. Leonhardt. *Measuring the Quantum State of Light*. Cambridge University Press, 1997.

[28] U. Leonhardt. Quantum statistics of a lossless beam splitter: SU(2) symmetry in phase space. *Physical Review A*, 48(4):3265–3277, 1993.

[29] R. A. Campos, B. E. A. Saleh, and M. C. Teich. Quantum-mechanical lossless beam splitter: SU(2) symmetry and photon statistics. *Physical Review A*, 40(3):1371–1384, 1989.

[30] V. Parigi, A. Zavatta, and M. Bellini. Implementation of single-photon creation and annihilation operators: experimental issues in their application to thermal states of light. *Journal of Physics B: Atomic, Molecular and Optical Physics*, 42(11):114005, 2009.

[31] R. H. Hadfield. Single-photon detectors for optical quantum information applications. *Nature Photonics*, 3(12):696–705, 2009.

[32] G. S. Buller and R. J. Collins. Single-photon generation and detection. *Measurement Science and Technology*, 21(1):012002, 2010.

[33] H. Iams and B. Salzberg. The secondary emission phototube. *Proceedings of the Institute of Radio Engineers*, 23(1):55 – 64, 1935.

[34] Y. Li, G. Li, Y. C. Zhang, X. Y. Wang, J. Zhang, J. M. Wang, and T. C. Zhang. Effects of counting rate and resolution time on a measurement of the intensity correlation function. *Physical Review A*, 76(1):013829, 2007.

[35] Y. Li, Y.-C. Zhang, P.-F. Zhang, Y.-Q. Guo, G. Li, J.-M. Wang, and T.-C. Zhang. Experimental study on coherence time of a light field with single photon counting. *Chinese Physics Letters*, 26(7):074205, 2009.

[36] R. E. Warburton, A. McCarthy, A. M. Wallace, S. Hernandez-Marin, S. Cova, R. A. Lamb, and G. S. Buller. Enhanced performance photon-counting time-of-flight sensor. *Opt. Express*, 15(2):423–429, 2007.

[37] A. Zavatta, V. Parigi, M. S. Kim, and M. Bellini. Subtracting photons from arbitrary light fields: experimental test of coherent state invariance by single-photon annihilation. *New Journal of Physics*, 10(12):123006, 2008.

[38] A. Ourjoumtsev, F. Ferreyrol, R. Tualle-Brouri, and P. Grangier. Preparation of non-local superpositions of quasi-classical light states. *Nature Physics*, 5(3):189–192, 2009.

[39] J. S. Lundeen, A. Feito, H. Coldenstrodt-Ronge, K. L. Pregnell, Ch. Silberhorn, T. C. Ralph, J. Eisert, M. B. Plenio, and I. A. Walmsley. Tomography of quantum detectors. *Nature Physics*, 5(1):27–30, 2009.

[40] A. Zavatta, S. Viciani, and M. Bellini. Non-classical field characterization by high-frequency, time-domain quantum homodyne tomography. *Laser Physics Letters*, 3(1):3–16, 2006.

[41] C. Silberhorn. Detecting quantum light. *Contemporary Physics*, 48(3):143–156, 2007.

[42] A. Zavatta, V. Parigi, M. S. Kim, H. Jeong, and M. Bellini. Experimental demonstration of the bosonic commutation relation via superpositions of quantum operations on thermal light fields. *Physical Review Letters*, 103(14):140406, 2009.

[43] F. Ferreyrol, M. Barbieri, R. Blandino, S. Fossier, R. Tualle-Brouri, and P. Grangier. Implementation of a nondeterministic optical noiseless amplifier. *Physical Review Letters*, 104(12):123603, 2010.

[44] X. Maitre, E. Hagley, G. Nogues, C. Wunderlich, P. Goy, M. Brune, J. M. Raimond, and S. Haroche. Quantum memory with a single photon in a cavity. *Physical Review Letters*, 79(4):769–772, 1997.

[45] S. Gleyzes, S. Kuhr, C. Guerlin, J. Bernu, S. Deleglise, U. B. Hoff, M. Brune, J.-M. Raimond, and S. Haroche. Quantum jumps of light recording the birth and death of a photon in a cavity. *Nature*, 446:297–300, 2007.

[46] S. Deleglise, I. Dotsenko, C. Sayrin, J. Bernu, M. Brune, J.-M. Raimond, and S. Haroche. Reconstruction of non-classical cavity field states with snapshots of their decoherence. *Nature*, 455(7212):510–514, 2008.

[47] B. T. H. Varcoe, S. Brattke, and H. Walther. The creation and detection of arbitrary photon number states using cavity QED. *New Journal of Physics*, 6, 2004.

[48] C. Guerlin, J. Bernu, S. Deleglise, C. Sayrin, S. Gleyzes, S. Kuhr, M. Brune, J.-M. Raimond, and S. Haroche. Progressive field-state collapse and quantum non-demolition photon counting. *Nature*, 448:889–893, 2007.

[49] N. Imoto, M. Ueda, and T. Ogawa. Microscopic theory of the continuous measurement of photon number. *Physical Review A*, 41(7):4127–4130, 1990.

[50] P. Bhattacharya. *Semiconductor Optoelectronic Devices*. Prentice-Hall, second edition, 1997.

[51] J. Singh. *Semiconductor Optoelectronics: Physics and Technology*. McGraw-Hill, 1995.

[52] P. L. Kelley and W. H. Kleiner. Theory of electromagnetic field measurement and photoelectron counting. *Physical Review*, 136(2A):A316–A334, 1964.

[53] M. D. Srinivas and E. B. Davies. Photon counting probabilities in quantum optics. *Journal of Modern Optics*, 28(7):981–996, 1981.

[54] C. T. Lee. External photodetection of cavity radiation. *Physical Review A*, 48(3):2285–2291, 1993.

[55] M. Ueda, N. Imoto, and T. Ogawa. Quantum theory for continuous photodetection processes. *Physical Review A*, 41(7):3891–3904, 1990.

[56] M. C. de Oliveira, S. S. Mizrahi, and V. V. Dodonov. A consistent model for continuous photodetection processes. *Journal of Optics B: Quantum and Semiclassical Optics*, 5:S271–S280, 2003.

[57] A. V. Dodonov, S. S. Mizrahi, and V. V. Dodonov. Quantum photodetection distributions with 'nonlinear' quantum jump superoperators. *Journal of Optics B: Quantum and Semiclassical Optics*, 7:99–108, 2005.

[58] H. Fearn. Linear amplifiers and attenuators. *Quantum Optics: Journal of the European Optical Society Part B*, 2(2):103, 1990.

[59] D. Achilles, C. Silberhorn, C. Sliwa, K. Banaszek, I. A. Walmsley, M. J. Fitch, B. C. Jacobs, T. B. Pittman, and J. D. Franson. Photon-number-resolving detection using time-multiplexing. *Journal of Modern Optics*, 51(9):1499–1515, 2004.

[60] A. V. Dodonov, S. S. Mizrahi, and V. V. Dodonov. Microscopic models of quantum-jump superoperators. *Physical Review A*, 72:023816, 2005.

[61] S. S. Mizrahi, A. V. Dodonov, and V. V. Dodonov. Comparison between different models for quantum jump superoperators in cavity QED experiments. *Journal of Russian Laser Research*, 30:485–492, 2009.

[62] A. V. Dodonov, S. S. Mizrahi, and V. V. Dodonov. Engineering quantum jump superoperators for single-photon detectors. *Physical Review A*, 74(3):033823, 2006.

[63] A. V. Dodonov, S. S. Mizrahi, and V. V. Dodonov. Inclusion of nonidealities in the continuous photodetection model. *Physical Review A*, 75(1):013806, 2007.

[64] T. Häyrynen, J. Oksanen, and J. Tulkki. General photon counting model for beam splitters and optoelectronic devices. 2009 MRS Fall Meeting Proceedings, 2010. 1229-LL05-10.

[65] C. T. Lee. Superoperators and their implications in the hybrid model for photodetection. *Physical Review A*, 49(6):4888–4894, 1994.